REVIEW ARTICLE | OCTOBER 25 2023

Non-volatile materials for programmable photonics 🕞

Zhuoran Fang 🆔 ; Rui Chen 🆔 ; Bassem Tossoun 🆔 ; Stanley Cheung 🆔 ; Di Liang 🆔 ; Arka Majumdar ✉ 🆔

⬤ Check for updates

🌐 View Online

📄 Export Citation

CrossMark

Articles You May Be Interested In

A programmable ferroelectric single electron transistor

Appl. Phys. Lett. (February 2013)

Analysis Of Volatile Fingerprints: A Rapid Screening Method For Antifungal Agents For Efficacy Against Dermatophytes

AIP Conference Proceedings (May 2009)

A hybrid magnetic/complementary metal oxide semiconductor three-context memory bit cell for non-volatile circuit design

J. Appl. Phys. (April 2014)

Non-volatile materials for programmable photonics Ⓕ

View Online   Export Citation   CrossMark

Zhuoran Fang,[1,a)] Ⓘ Rui Chen,[1] Ⓘ Bassem Tossoun,[2] Ⓘ Stanley Cheung,[2] Ⓘ Di Liang,[2] Ⓘ
and Arka Majumdar[3,b)] Ⓘ

AFFILIATIONS

[1] Department of Electrical and Computer Engineering, University of Washington, Seattle, Washington 98195, USA
[2] Hewlett Packard Labs, Hewlett Packard Enterprise, Milpitas, California 95305, USA
[3] Department of Physics, University of Washington, Seattle, Washington 98195, USA

[a)]**Email:** rogefzr@uw.edu
[b)]**Author to whom correspondence should be addressed:** arka@uw.edu

ABSTRACT

Programmable photonics play a crucial role in many emerging applications, from optical accelerators for machine learning to quantum information technologies. Conventionally, photonic systems are tuned by mechanisms such as the thermo-optic effect, free carrier dispersion, the electro-optic effect, or micro-mechanical movement. Although these physical effects allow either fast (>100 GHz) or large contrast (>60 dB) switching, their high static power consumption is not optimal for programmability, which requires only infrequent switching and has a long static time. Non-volatile materials, such as phase-change materials, ferroelectrics, vanadium dioxide, and memristive metal oxide materials, can offer an ideal solution thanks to their reversible switching and non-volatile behavior, enabling a truly "set-and-forget" programmable unit with no static power consumption. In recent years, we have indeed witnessed the fast adoption of non-volatile materials in programmable photonic systems, including photonic integrated circuits and free-space meta-optics. Here, we review the recent progress in the field of programmable photonics, based on non-volatile materials. We first discuss the material's properties, operating mechanisms, and then their potential applications in programmable photonics. Finally, we provide an outlook for future research directions. The review serves as a reference for choosing the ideal material system to realize non-volatile operation for various photonic applications.

INTRODUCTION

Programmability is an increasingly important feature in modern-day photonic systems and is crucial to enabling technologies ranging from photonic accelerators for machine learning[1] to quantum information processing.[2] Such programmability is generally achieved by traditional modulation methods, including thermo-optic (TO),[3] free-carrier dispersion,[4] electro-optic (EO),[5] or mechanical tuning.[6] These physical effects either incur a large static power consumption (>10 mW in the case of the TO effect) or require a constant bias (in the case of the EO effect and mechanical tuning) when the photonic systems are in the standby state. Since the programmability only requires infrequent switching (normally <1 kHz) and the photonic systems stay in the standby state

most of the time, the static energy consumption can easily scale with the number of photonic switches and tremendously increase the power budget of the entire photonic system. The second major challenge faced by programmable photonics is that fabrication variation inevitably results in phase errors in the systems, particularly for high-index-contrast platforms such as silicon-on-insulators.[7] While wider or thicker waveguides and Si_3N_4 platforms have been proposed to improve the fabrication tolerance,[7] the most effective solution so far has been the use of TO phase shifters to correct phase errors in the resonators or interferometers. This will further incur large static power consumption and thermal crosstalk since these phase shifters are always in the on state. Therefore, by reducing or even removing such static power consumption, we can drastically improve the energy efficiency and reduce the crosstalk of any

26 October 2023 02:57:41

programmable photonic systems, including routing light in optical interconnects,[8] setting phase masks in spatial light modulators (SLMs),[9] semi-static displays,[10] or trimming photonic resonators to the same resonance frequency.[11,12] In fact, this can be readily achieved by using non-volatile tuning mechanisms where the optical state can be maintained without any power consumption or bias, akin to a "set-and-forget" switch. Non-volatile materials, such as phase-change materials (PCMs), memristive materials, ferroelectric materials, and ferromagnetic materials, are attractive candidates to realize non-volatile tuning as they have proven to be reliable memory mediums in electronics and optical storage. For example, PCMs

are the enabling technology behind rewritable compact disks[13] and phase-change random access memory (RAM);[14] Memristive materials are the building blocks of Resistive RAM (ReRAM);[15] Ferroelectric RAM (FeRAM) and ferroelectric field effect transistors (FeFETs) are based on ferroelectric materials;[16] and ferromagnetic materials are the key elements for magnetoresistive RAM (MRAM).[17] One exception is flash memory, which involves only CMOS compatible materials, normally thin tunneling dielectrics and a charge-trapping silicon layer, to achieve the desired memory effect.[18] Figure 1 shows the timeline of the development of various non-volatile material platforms for programmable photonics and memory applications. A
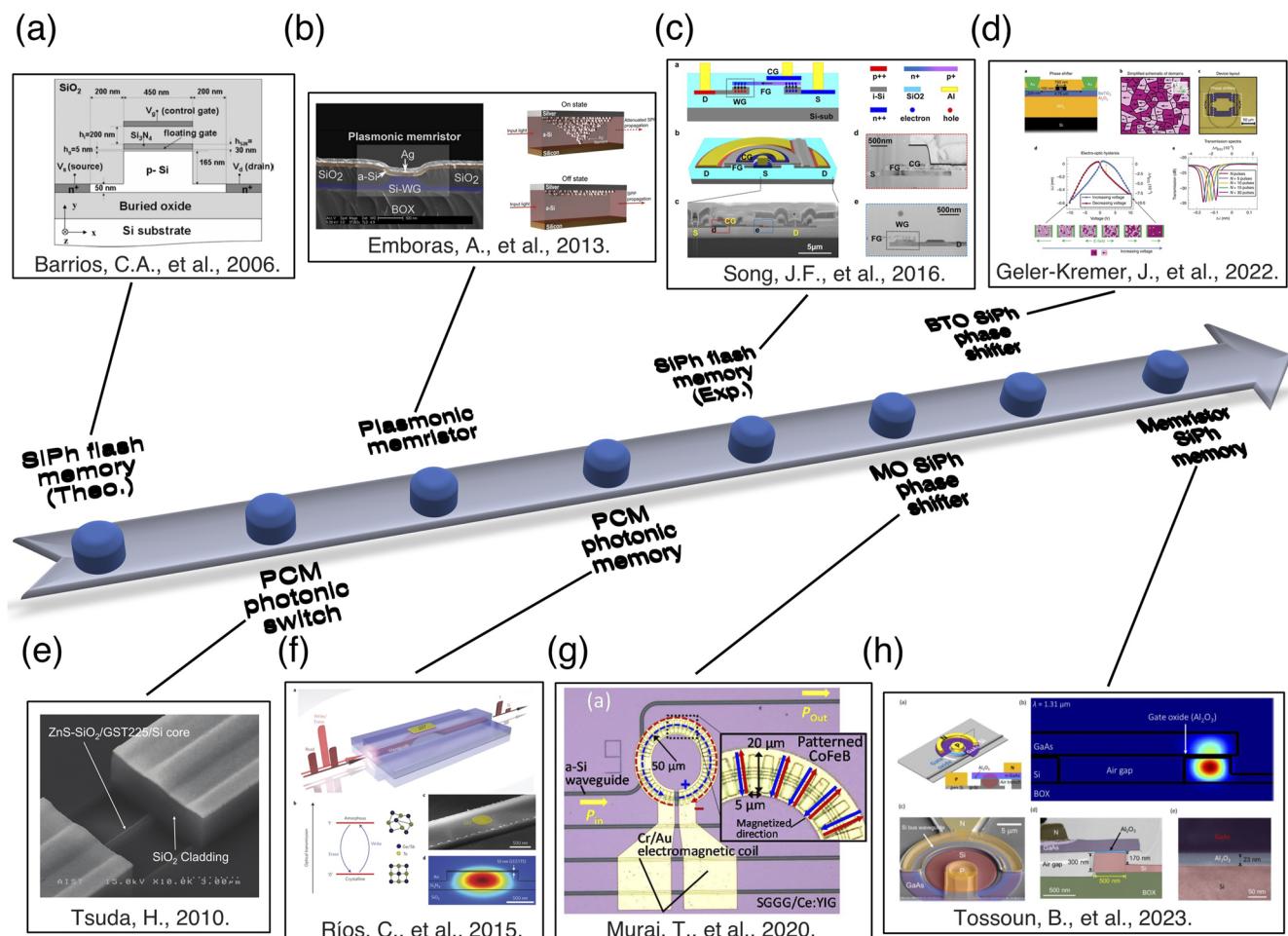
FIG. 1. Development of non-volatile materials for programmable photonics and memory. Here we depict the development of various non-volatile materials for photonic applications from 2006 to the present, including phase-change materials, flash memory, memristors, magneto-optic materials, and ferroelectric materials. SiPh (silicon photonics); PCM (phase-change material); MO (magneto-optic); BTO (Barium Titanate); Theo. (Theory); Exp. (Experiment). (a) is reprinted with permission from Barrios and Lipson, J. Lightwave Technol. **24**, 2898 (2006). Copyright 2006 IEEE. (b) is reprinted with permission from Emboras *et al.*, Nano Lett. **13**, 6151 (2013). Copyright 2013 American Chemical Society. (c) is reprinted with permission from Song *et al.*, Sci. Rep. **6**, 22616 (2016). Copyright 2016 Author(s), licensed under a Creative Commons Attribution 4.0 License. (d) is reprinted with permission from Geler-Kremer, J., *et al.*, Nat. Photonics **16**, 491 (2022). Copyright 2022 Springer Nature. (e) is From Tsuda, Asia Communications and Photonics Conference and Exhibition. Copyright 2010 IEEE. Reprinted with permission from IEEE. (f) is reprinted with permission from Ríos *et al.*, Nat. Photonics **9**, 725 (2015). Copyright 2015 Nature Publishing Group. (g) is reprinted with permission from Murai *et al.*, Opt. Express **28**, 31675 (2020). Copyright 2020 Optical Society of America. (h) is reprinted with permission from Tossoun *et al.*, ■ ■, ■ (2023). Copyright 2023 Author(s), licensed under a Creative Commons Attribution 4.0 License.

26 October 2023 02:57:41

silicon nanocrystal optical memory was first demonstrated in 2004 based on the charge-trapping effect,[19] which is read optically via the nanocrystals' photoluminescence into free space. Photonic integration of charge-trapping flash memory onto silicon waveguides was first theoretically proposed[20] in 2006 and demonstrated experimentally ten years later.[21] On the other hand, PCMs were first proposed to be used for optical switching in a silicon waveguide in 2010[22] and later in integrated photonic memory[23] and optical computing.[24] A photonic memristor based on amorphous silicon was first demonstrated in 2013.[25] More recently, III–V-on-Si photonic memristors have been studied in non-volatile tunable lasers[26] and silicon photonic memory.[27–31] Active photon sources were discovered in an Ag/amorphous-SiO/Pt plasmonic memristor.[32] A non-volatile magneto-optic silicon photonic phase shifter based on ferromagnetic CoFeB was reported in 2020.[33] Ferroelectric materials such as Barium Titanate (BTO) have recently enabled a multilevel non-volatile silicon photonic phase shifter.[34] Finally, vanadium dioxide (VO$_2$), a material previously considered to be volatile, was recently discovered to exhibit a memory effect under a constant voltage bias.[35] Due to the rising interest in this field, in this article, we review the recent progress in the applications of non-volatile materials in programmable photonics and optical memory. We first explain the underlying mechanisms responsible for the non-volatile effect in these materials and then compare their key performance metrics, such as switching speed, endurance, and switching energy, before discussing their suitability for various photonic applications. Several future research directions are also identified. The article aims to serve as a general guideline for researchers who are looking for the most suitable non-volatile material systems for their desired photonic applications. Note that here, we limit our discussion to long-term non-volatile effects (expected > 10 years of retention time) instead of short-term optical bistability commonly based on nonlinearity (<10 s of retention time), which requires a constant optical bias to operate.[36–39] The latching effect of micro-electromechanical systems (MEMS) can also enable non-volatile photonic switching[40] but is out of the current scope, which focuses mainly on the non-volatile property of the photonic material.

PHASE-CHANGE MATERIALS AND PHASE-CHANGE MEMORY

Phase-change materials (PCMs), exemplified by Ge$_2$Sb$_2$Te$_5$ (GST), are chalcogenides that can be switched between bistable micro-structural states—crystalline and amorphous states. Figure 2 shows that to turn the materials from an ordered crystalline state to a disordered amorphous state, we apply a high power and short excitation to the PCMs that essentially melt-quench the materials into the amorphous state. The high-power excitation raises the material temperature above the melting point, and the short duration ensures it is cooled rapidly after the excitation is removed. To return the material to the crystalline state, a moderate amplitude and long excitation a applied that anneal the material into the crystalline state. The moderate power raises the material temperature above the crystallization temperature and below the melting point, and the long duration facilitates the long-range diffusion of atoms to settle into their most thermodynamically favorable crystalline state. Such thermal excitation can be achieved either via optical or electrical pulses. Since crystalline PCM has a higher refractive index than its amorphous
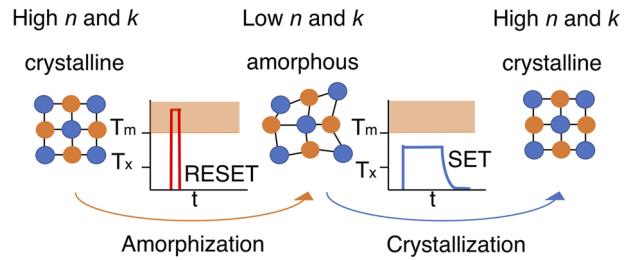

FIG. 2. Operating principle of phase-change materials in programmable photonics. PCMs tend to have a higher refractive index in the crystalline state due to the *meta*-valent bonding,[50] and a lower index in the amorphous state due to the covalent bonding. A high amplitude and short excitation are applied to switch the PCM into the disordered amorphous state. The excitation melts the material before quenching it rapidly to prevent long-range diffusion. To return the material to its crystalline state, a moderate amplitude and long excitation are used to anneal the material into an ordered crystalline state. For programmable photonics, typically ~100 mW of power and ~100 ns pulse width are required for RESET.[51] For SET, the power is ~10 mW and the pulse width is around tens of μs. However, the switching power and time do scale with the volume of the PCMs and can go down to only ~μW and ~ns in nanoscale electronic memory.[52] n (refractive index); k (extinction coefficient); T_m (melting point); T_x (crystallization temperature).

state due to the increased electron delocalization,[41] we can harness such a large refractive index contrast (typically Δn >1) to control the phase and absorption of the light propagating inside the material.[42] In the early days, PCMs were widely used in rewritable compact disks to store data. They were typically designed to be highly absorptive at the visible wavelength so that they could be easily switched by laser pulses. Later, they found applications in electronic memory, where data are stored in the high and low resistance of the memory cell, rendering the optical absorption of the materials entirely irrelevant. It is only recently, with the advent of PCM-integrated photonics,[43,44] that absorptive loss has become critical. The proximity of the PCMs to the optical mode in a waveguide can lead to a significant loss even for a very short PCM segment, e.g., 10 nm crystalline GST typically gives >1 dB/μm insertion loss on a Si$_3$N$_4$ waveguide.[45] To address this issue, new PCMs have been discovered that have wider bandgaps and hence lower losses than GST,[46] such as GSST,[47] GSSe,[47] Sb$_2$Se$_3$,[48] and Sb$_2$S$_3$.[48,49]

APPLICATIONS OF PHASE-CHANGE MATERIALS IN PHOTONICS

We categorize the applications of PCMs into four quadrants depending on whether they are intended for free space or photonic integrated circuits (PICs) and whether the control is via electrical or optical means (see Fig. 3). The earliest work can be traced back to Tsuda, who first used a laser to switch Ge$_2$Sb$_2$Te$_5$ (GST) on a silicon waveguide and demonstrated an ultra-compact optical switch.[22] The same group improved on their previous design to show a selfholding optical switch based on a multi-mode Si waveguide that can be reversibly switched over 2000 cycles.[53] Rudé *et al.* first showed the control of a microring by laser switching GST[54] [Fig. 3(b-i)]. The use of microrings was later improved by Zheng *et al.,* who achieved 33 dB extinct ratio contrast via critical coupling[42] Fig. 3(b-ii)] and quasi-continuous operation depending on the number of applied laser pulses. Rios *et al.* first showed that optical excitation can be
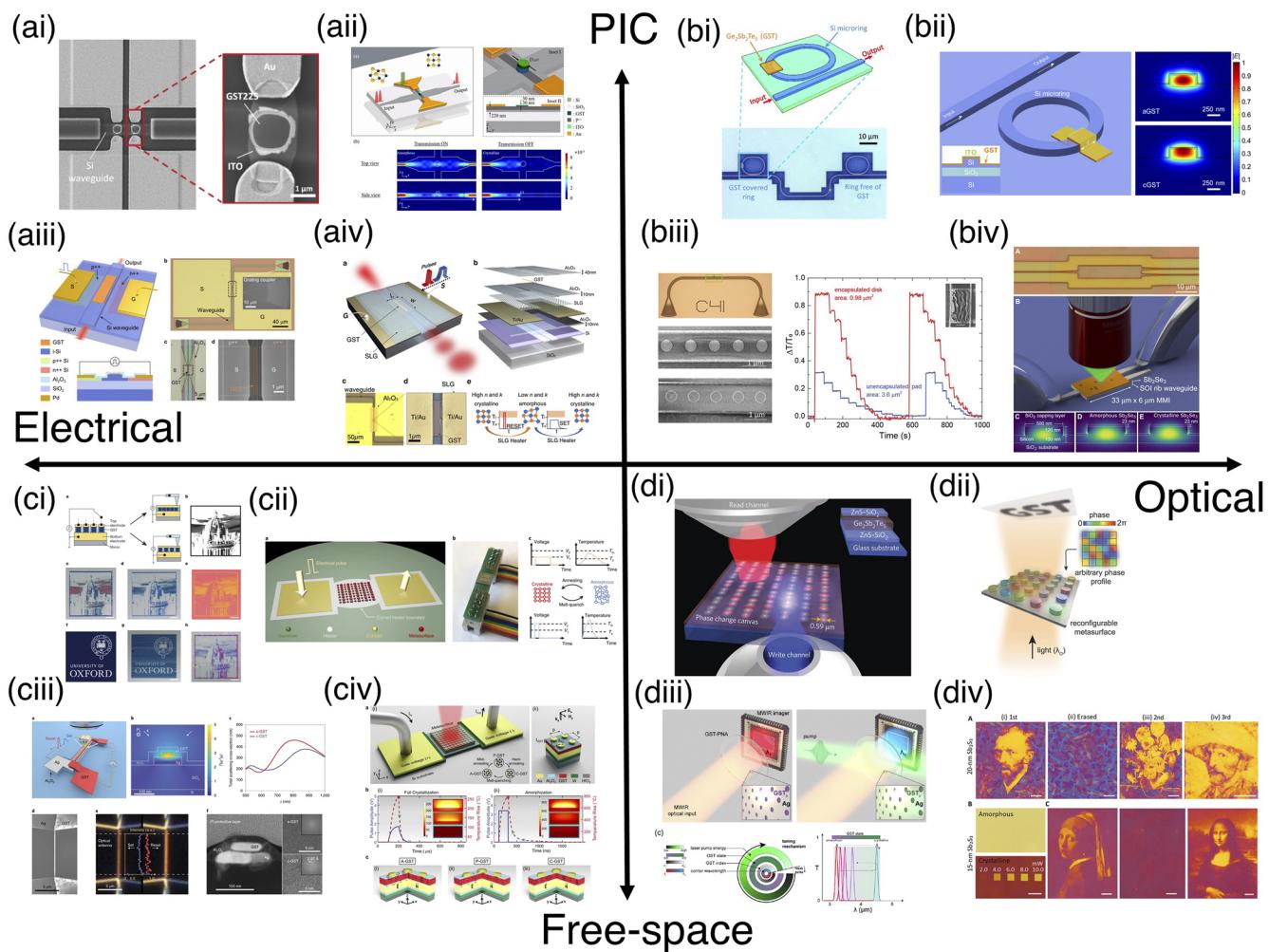
FIG. 3. Applications of phase-change materials in photonics. (a-i) Si photonic switch based on GST and ITO microheater.[58] (a-ii) Silicon photonic switch based on a doped multi-mode waveguide microheater and GST.[59] (a-iii) Silicon photonic switch based on PIN diode microheater and GST.[51] (a-iv) Silicon photonic switch based on graphene microheater for controlling both GST and Sb_2Se_3.[60] (b-i) Optical switching of GST in a racetrack resonator.[54] (b-ii) High extinction ratio switching of GST in a microring.[42] (b-iii) On-chip optical switching of subwavelength patterned GST.[55] (b-iv) Optical switching of Sb_2Se_3 demonstrating 2π phase shift in MZIs.[56] (c-i) Electrically tunable reflective display based on GST.[10] (c-ii) Electrically reconfigurable metasurfaces based on GSST.[62] (c-iii) Electrically reconfigurable plasmonic metasurface based on GST.[63] (c-iv) Electrically reconfigurable plasmonic metasurfaces based on GST with a large modulation depth (80%).[64] (d-i) Optically reconfigurable metasurfaces based on GST.[65] (d-ii) Optically programmable Huygens' metasurface based on GST demonstrating near 2π phase shift in mid-IR.[66] (d-iii) Optically tunable mid-IR spectral filter based on GST.[67] (d-iv) Rewritable color nanoprint based on Sb_2S_3 using femtosecond laser.[68] (a-i) is reprinted with permission from Kato *et al.*, Appl. Phys. Express **10**, 072201 (2017). Copyright 2017 The Japan Society of Applied Physics. (a-ii) is reprinted with permission form Zhang *et al.*, ACS Photonics **6**, 2205 (2019). Copyright 2019 American Chemical Society. (a-iii) is reprinted with permission from Zheng *et al.*, Adv. Mater. **32**, 2001218 (2020). Copyright 2020 Wiley-VCH. (a-iv) is reprinted with permission from.[60] Copyright 2022 Author(s), licensed under a Creative Commons Attribution 4.0 License. (b-i) is reprinted from Rudé *et al.*, Appl. Phys. Lett. **103**, 141119 (2013) with the permission of AIP Publishing. (b-ii) is reprinted with permission from Zheng *et al.*, Opt. Mater. Express **8**, 1551 (2018). Copyright 2018 Optical Society of America. (b-iii) is reprinted with permission from Wu *et al.*, ACS Photonics **6**, 87 (2019).Copyright 2018 American Chemical Society. (b-iv) is reprinted with permission from Delaney *et al.*, Sci. Adv. **7**, eabg3500 (2021). Copyright 2021 Author(s), licensed under a Creative Commons Attribution 4.0 License. (c-i) is reprinted with permission from Hosseini *et al.*, Nature **511**, 206 (2014). Copyright 2014 Nature Publishing Group. (c-ii) is reprinted with permission from Zhang *et al.*, Nat. Nanotechnol. **16**, 661 (2021). Copyright 2021 Author(s), licensed under a Creative Commons Attribution 4.0 License. (c-iii) is reprinted with permission from Wang *et al.*, Nat. Nanotechnol. **16**, 667 (2021). Copyright 2021 Author(s), licensed under a Creative Commons Attribution 4.0 License. (c-iv) is reprinted with permission from Abdollahramezani *et al.*, Nat. Commun. **13**, 1696 (2022). Copyright 2022 Author(s), licensed under a Creative Commons Attribution 4.0 License. (d-i) is reprinted with permission from Wang *et al.*, Nat. Photonics **10**, 60 (2016).Copyright 2016 Nature Publishing Group. (d-ii) is reprinted with permission from Leitis *et al.*, Adv. Funct. Mater. **30**, 1910259 (2020). Copyright 2020 Wiley-VCH. (d-iii) is reprinted with permission from Williams *et al.*, Optica **7**, 746 (2020). Copyright 2020 Optical Society of America. (d-iv) is reprinted with permission from Liu *et al.*, Sci. Adv. **6**, eabb7171 (2020). Copyright 2020 Author(s), licensed under a Creative Commons Attribution 4.0 License.

coupled into a waveguide for switching PCMs and demonstrated a multilevel photonic memory.[23] Wu *et al.* showed that by patterning the PCMs on subwavelength scales and using atomic-layer-deposited Al_2O_3 as encapsulation, the switching contrast can be significantly improved by almost threefold[55] [Fig. 3(b-iii)]. Apart from GST, it has been shown recently that low-loss PCMs Sb_2Se_3 can also be controlled by a laser in a Mach–Zehnder interferometer where 2π phase-only modulation has been achieved[56] [Fig. 3(b-iv)]. Although optical switching can reduce the difficulty of fabrication, a truly scalable photonic platform requires electrical switching,[44,57] which harnesses the mature CMOS technology that enables the integration of billions of transistors on a single chip. Kato *et al.* first used the ITO microheater to electrically control GST on the Si waveguide[58] [Fig. 3(a-i)], while Zhang *et al.* doped the Si waveguide to create microheaters[59] [Fig. 3(a-iii)]. The doped Si microheater was later modified into a PIN diode microheater that significantly reduces the loss from doping[51] [Fig. 3(a-iii)]. More recently, graphene was also shown to be a reliable and energy efficient microheater for the electrical control of PCMs on various materials and substrates, including Si[60] and SiO_2.[61] [Fig. 3(a-iv)].

Beyond PICs, PCMs also find applications in free space. Early work envisioned an electrically tunable reflective display based on GST where each pixel can be individually switched using ITO electrodes[10] [Fig. 3(c-i)]. Such a rewritable color nanoprint has also been achieved in wide bandgap PCMs Sb_2S_3 controlled by a femtosecond laser[68] [Fig. 3(d-iv)]. Wang *et al.* first demonstrated an optically reconfigurable metasurface where they showed phase masks of zone plates and gratings, etc. can be written into a blanket thin film of GST[65] [Fig. 3(d-i)]. Using Huygen's metasurface, near 2π phase control was realized[66] [Fig. 3(d-iii)]. A tunable spectral filter in the mid-IR was demonstrated using a GST-Ag plasmonic metasurface.[67] Similar functionalities such as spectral tuning and beam steering were also demonstrated using metasurfaces via electrical control by metallic microheaters in visible and near IR[62-64] [Figs. 3(c-ii)–3(c-iv)]. For a more detailed discussion, please also refer to other review papers on PCM-based photonics.[43,44,69]

MEMRISTORS AND RESISTIVE MEMORY

A memristor consists of a metal-dielectric-metal or semiconductor-dielectric-semiconductor tri-layer (see Fig. 4). Typical choices of metals include Pt, Ti, Ta, and Al, and the dielectrics are oxides such as TiO_2, NiO, Al_2O_3, HfO_2, TaO_2, etc. Note that the top and bottom metal or semiconductor layers do not have to be identical and are typically chosen to aid the process of catalyzing anions or cations in the memristors.[70] At moderate bias across the junction, the material stack acts as a capacitor. Beyond a certain threshold voltage, the ions inside the dielectric, for example, oxygen ions inside transitional metal oxides,[71,72] start to migrate toward the anode. In some situations, metal ions from the electrodes, for example, Ta cations from the Ta electrodes,[73] start to migrate toward the cathode. If we consider the simple case of oxygen ion migration, then simultaneously, the oxygen vacancies migrate toward the cathode. A conduction filament (CF) is formed by the percolation of oxygen vacancies under a high electric field, and its growth is promoted by the subsequent Joule heating.[74] The first formation of the CFs in a pristine dielectric is called "electroforming," which brings the memristor to the low resistance state (LRS). It generates defects inside the dielectric and makes subsequent switching of the memristor possible. Once the CF forms, the memristor can be reset by reversing the bias polarity in the case of bipolar switching or using the same polarity in the case of unipolar switching. The RESET causes the rupture of the CFs due to a combined effect of Joule heating and an electric field.[75] For bipolar switching (depicted in Fig. 4), it is believed that the electric field plays a more significant role in CF rupture, while for unipolar switching, Joule heating seems to play a more dominant role.[75] The breaking of CFs brings the memristor to the high resistance state (HRS). Instead of dissolving the entire CF, the RESET normally causes the breaking of CF only at the thinnest section, where the resistance is the largest.[72] Hence, to set the memristor back to the LRS, a lower voltage is required than the electroforming to reconnect the CF. The memristor can be
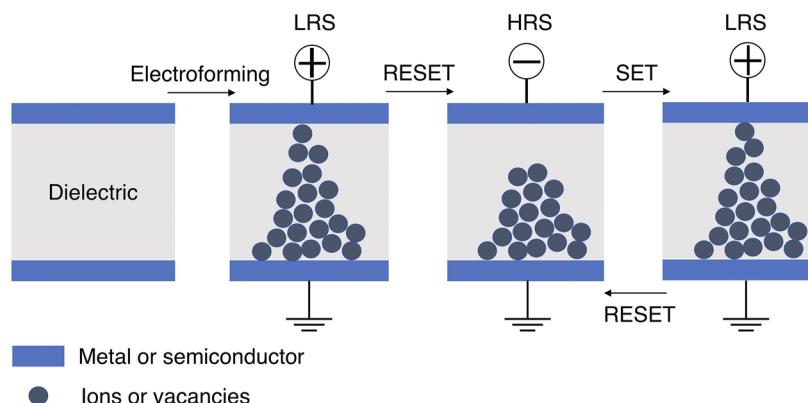
FIG. 4. Operating principle of a memristor under bipolar switching. A memristor typically consists of a conductor-insulator-conductor tri-layer. The conductors can be either metals or semiconductors while the insulator is generally dielectric materials. A conduction filament is formed by applying a large enough voltage which switches the memristor from the initial HRS into the LRS. This process is called "electroforming." The memristor can be returned to the HRS by reversing the bias polarity which breaks the filaments. The switching is reversible and non-volatile as the filament remains after the bias is removed. Since the conduction filaments do not break completely during RESET, the SET normally require lower voltage than the electroforming. LRS (HRS), low resistance state (high resistance state).

reversibly switched between HRS and LRS for millions of cycles,[76] and the excitation can either be direct current (e.g., an IV sweep) or pulses. So far, two approaches have been studied to couple the memristive switching in the electronic domain to the optical domain. One can use a plasmonic waveguide to confine the optical mode inside the subwavelength thick dielectric layers, maximizing the overlap between the optical field maxima and the nanoscale filaments.[25,77–79] This approach leads to large optical contrast

(>10 dB) without the need for a read bias, but the insertion loss is high. The second approach is to combine memristive switching with the free carrier dispersion effect.[30,31] Under a small read bias, the free carriers will accumulate at the metal-oxide-semiconductor capacitor when the memristor is in the HRS and leak through the dielectric when the memristor is in the LRS. The advantage of this approach is that the plasmonic waveguides are no longer needed, and loss can be reduced, but a bias will be required to read the optical states.
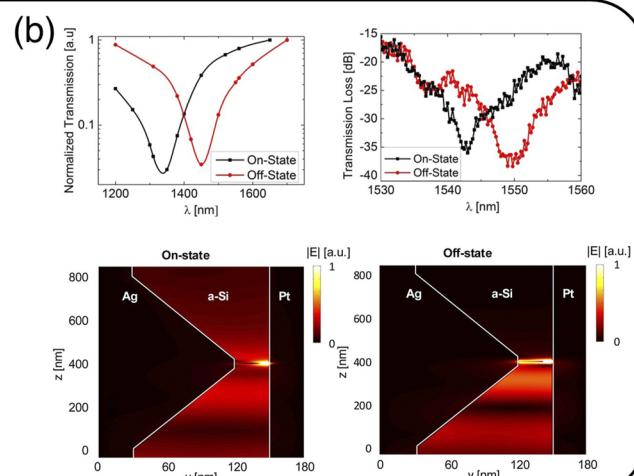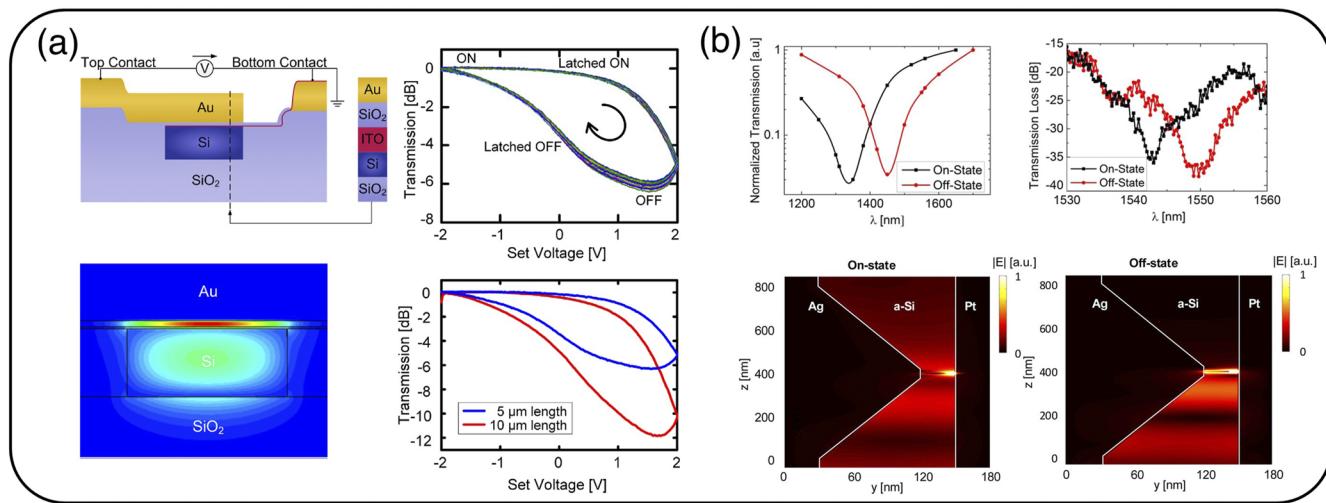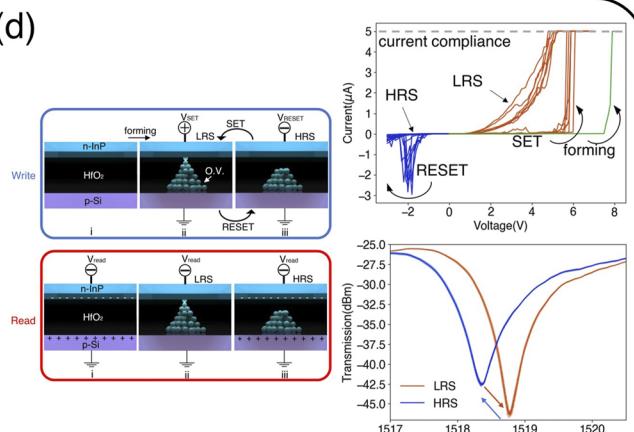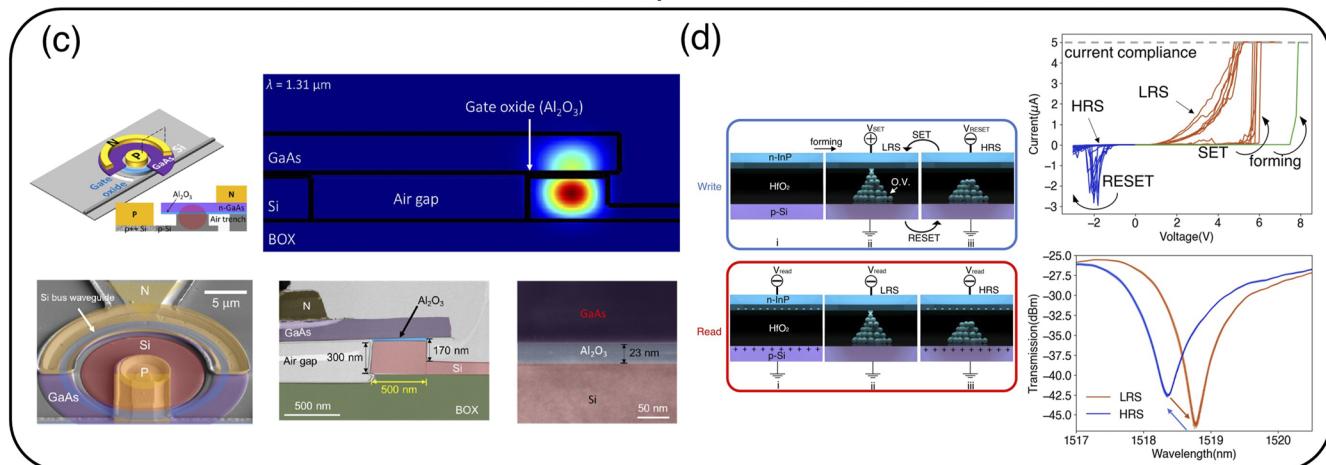
FIG. 5. Applications of memristors in programmable photonics. (a) A Au/SiO$_2$/ITO plasmonic memristor.[77] The plots show a clear hysteresis in optical transmission upon switching the plasmonic memristor on and off by sweeping the voltage. Extinction ratios of 12 dB are demonstrated in 10 μm devices at operating voltages of ± 2V. (b) Single-atom switching in a Ag/aSi/Pt plasmonic memristor.[78] Switching of the plasmonic resonance in the 1550 nm wavelength range is shown, leading to a large extinction ratio of 10 dB. (c) Silicon photonic memory based on an GaAs/Al$_2$O$_3$/Si memristor integrated with a microring resonator.[30] The TEM shows the heterogeneous integration of III–V materials with Si and a 20 nm bonding oxide layer in between. (d) Silicon photonic phase shifter based on an n-InP/HfO$_2$/p-Si memristor.[31] The I–V curve shows typical memristor switching in the electrical domain, while the transmission spectrum shows the switching of microring resonance in the optical domain. (a) is reprinted with permission from Hoessbacher et al., Optica **1**, 198 (2014). Copyright 2014 Optical Society of America. (b) is reprinted with permission from Emboras et al., Nano Lett. **16**, 709 (2016). Copyright 2016 American Chemical Society. (c) is reprinted with permission from Tossoun et al., ■ ■, ■ (2023). Copyright 2023 Author(s), licensed under a Creative Commons Attribution 4.0 License. (d) is reprinted with permission from Fang et al., ■ ■, ■ (2023). Copyright 2023 Author(s), licensed under a Creative Commons Attribution 4.0 License.

Such bias can be applied via ultra-short read pulses to reduce static power consumption.[80] Moreover, in the LRS state, the DC bias would lead to static power due to the finite leakage current. These two approaches will be discussed in detail in the section below.

APPLICATIONS OF MEMRISTORS IN PHOTONICS

A recent review paper has discussed the recent progress in various memristor technologies for photonic applications.[81] Here, we approach the same topic differently by separating the field into two main research directions, i.e., plasmonic and photonic memristors. Emboras *et al.* first proposed a plasmonic memristor in an Ag–Si plasmonic waveguide.[25] The memristive switching is caused by the formation and breaking of Ag filaments inside the amorphous Si dielectric [see Fig. 1(b)]. The subwavelength confinement of the plasmonic waveguide ensures maximal overlap between the mode and the nanoscale filaments. Based on a similar design logic, Fig. 5(a) shows an Au/SiO$_2$/ITO plasmonic memristor demonstrated by Hoessbacher *et al.* with 39% of the field confined in the SiO$_2$ layer, resulting in a large extinction ratio of 12 dB. It was further shown that only a few atoms are enough to trigger large extinction ratio switching (9.2 dB) in an Ag/Si/Pt plasmonic memristor[78] [see Fig. 5(b)]. Apart from optical switching, the plasmonic memristor can also be used for photodetection, where the atomic-scale filaments can be ruptured by a small increase in light intensity.[82] In addition, by evanescently coupling light from a Si waveguide

to a memristor, the linearity of the memristive switching can be enhanced by a factor of four compared to the absence of light radiation due to the increased oxygen vacancies and diffusion rate.[83] The near analog operation is shown to be beneficial for neuromorphic computing.[83] A recent study showed that memristors can act as photon source—the formation and dissolution of CFs will lead to the emission of photons—which can potentially be used as single photon emitters for quantum applications or light sources for optical communications.[32] Finally, it was discovered that the memristor can also tune the plasmonic scattering of visible light (~600 nm) from an Ag nanodot on an Au mirror.[84] This phenomenon can be used to uncover the morphological changes of the CFs during switching in a non-destructive way. Although plasmonic memristors can achieve large optical contrast by switching atomic scale nanofilaments, the high insertion loss (~10 dB for a 10 μm long device) can be prohibitive for large-scale PICs. More recently, a silicon photonic memristor based on heterogeneous integration of III–V materials onto a silicon waveguide was demonstrated with low insertion loss for the first time by Tossoun *et al.* (~0.05 dB for a 10 μm radius microring).[30] The memristor is formed by an n-type GaAs and a p-type Si sandwiching a thin layer of Al$_2$O$_3$ inside a microring resonator. Since the mode is largely confined inside the silicon [Fig. 5(c)], the loss is significantly reduced, but the formation of nano-filament does not couple very well to the optical domain due to the small mode overlap. To enhance the effect of memristive switching, a bias is normally applied across the
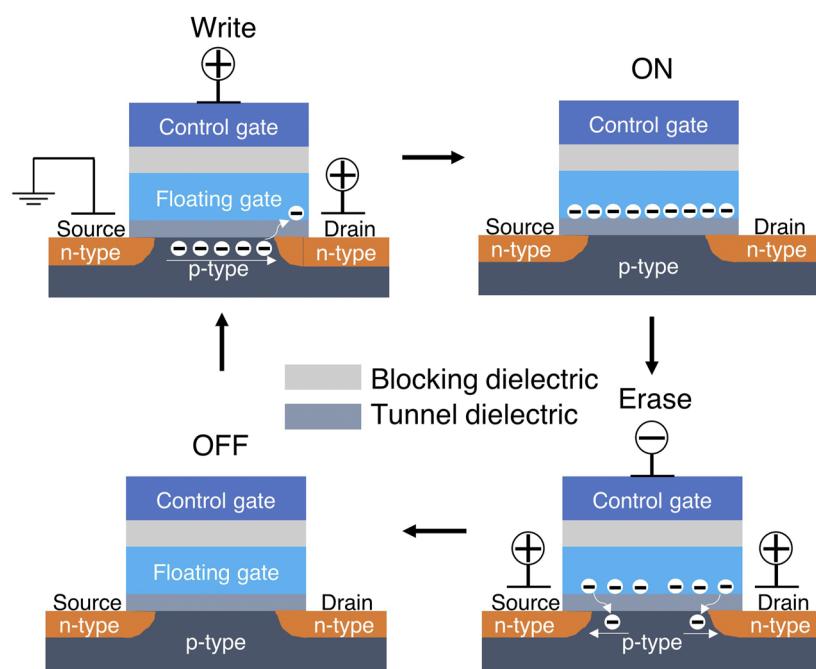
FIG. 6. Operating principle of flash memory. A flash memory cell is based on a traditional MOSFET configuration with an additional floating gate, typically made of polysilicon. Depending on the polarity of the gate voltage, the electrons can be shifted back and forth between the floating gate and the conduction channel via tunneling. The carriers are trapped inside the floating gate by the thin dielectric underneath it after the bias is removed, which provides the memory effect. This can be readily converted into a photonic memory by etching the p-type silicon into a waveguide. Light propagating within the waveguide will interact with the trapped charges via free carrier dispersion: strong dispersion when there are trapped charges and weak dispersion when there are no charges.

metal-oxide-semiconductor capacitor to optically read the resonance shift. The memristor switches the operating mode from capacitive carrier accumulation (spectral blue shift) to leakage-resulted carrier injection (spectral red shift), resulting in a difference in the resonance wavelength. Since the switching occurs at the nanoscale filament, the photonic memristor can be switched at high speed (300 ps) and consumes ultra-low energy (0.15 pJ). Based on a similar configuration, a non-volatile phase shifter has also been demonstrated with an n-type InP/HfO$_2$/p-type Si memristor[31,85] [see Fig. 5(d)]. The memristor is electrically written using pulses and optically read with a −3V bias, which results in a non-volatile shift in the microring resonance between the LRS and HRS. The

non-volatile phase shifter has a low switching energy of ~400 fJ with a L_π of ~0.5 mm.

FLASH MEMORY

Similar to memristors, flash memory also leverages the capacitive effect for switching. Flash memory is a non-volatile memory based on a floating gate MOSFET[18] (see Fig. 6). Compared to conventional MOSFETs, a floating gate (FG), which typically consists of polycrystalline Si, is inserted into the dielectric layer, typically made up of SiO$_2$, underneath the control gate (CG). Applying an ON-voltage to the CG will allow electrons to flow from the source
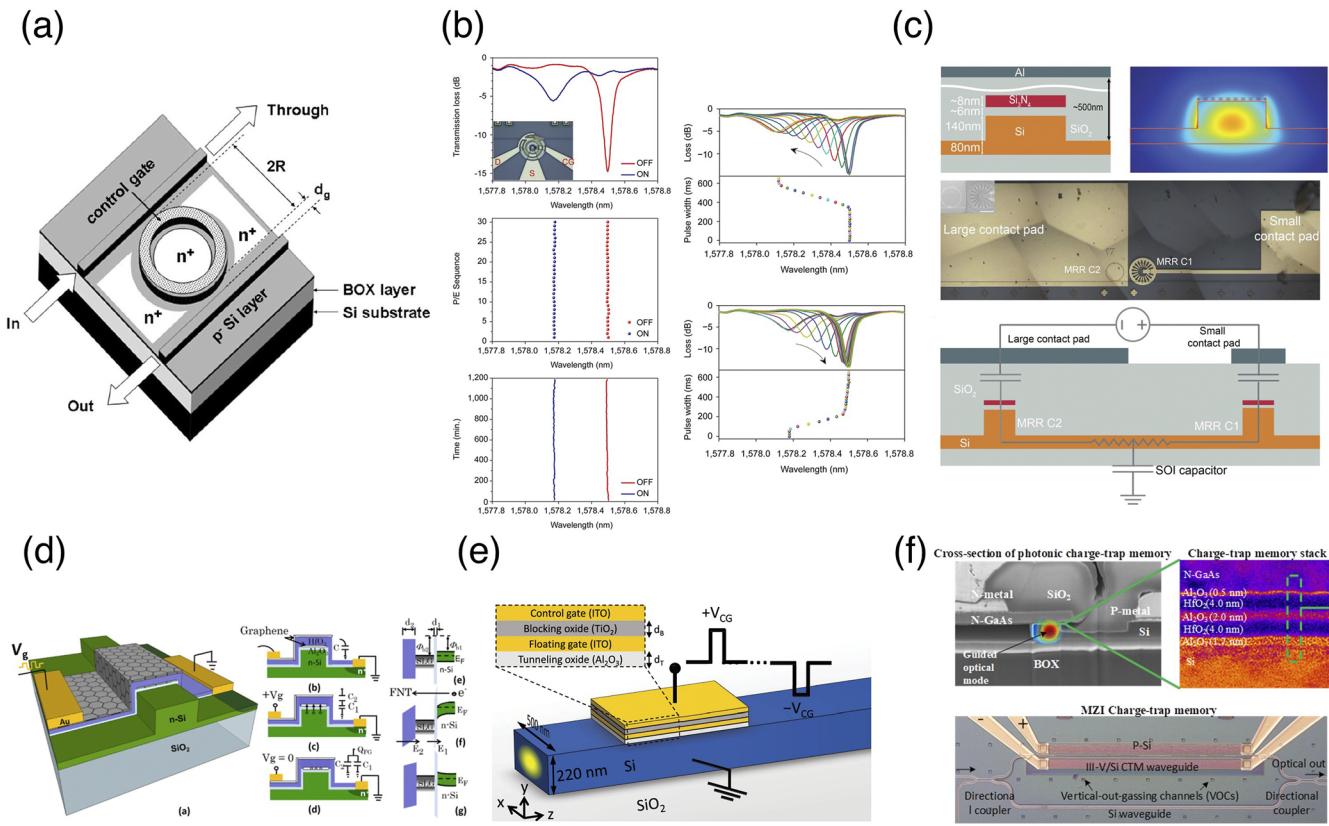

FIG. 7. Applications of flash memory in programmable photonics. (a) A silicon photonic read-only memory based on a Si$_3$N$_4$ floating gate.[20] A microring-based photonic memory was first proposed in simulation, which shows that optical information can be stored in different microring resonance states, controlled by the number of trapped charges. (b) Experimental demonstration of a multilevel programmable silicon photonic memory based on a poly-Si floating gate.[21] The resonance wavelengths of the on and off states were shown to be stable over 20 hours, and the device can be reversibly switched for 30 cycles. (c) An optically written silicon photonic flash-memory.[86] UV light is used to optically excite the free carriers into the Si$_3$N$_4$ floating gates. (d) A silicon photonic flash memory with a graphene floating gate.[87] Graphene can potentially give a larger effective index change per unit of trapped charges compared to poly-Si. (e) A silicon photonic memory with an ITO floating gate.[88] ITO can be doped by the trapped carriers into the epsilon-near-zero regime, where a large extinction ratio over 10 dB can be realized for a 5 μm long electro-absorption switch. (f) A III–V-on-Si photonic flash memory based on a Mach–Zehnder interferometer.[89] The dielectric layer consists of alternating layers of Al$_2$O$_3$ and HfO$_2$, as revealed by the TEM. The multilayer structures were shown to exhibit more reliable switching compared to pure Al$_2$O$_3$. (a) is reprinted with permission from Barrios and Lipson, J. Lightwave Technol. **24**, 2898 (2006). Copyright 2016 IEEE. (b) is reprinted with permission from Song *et al.*, Sci. Rep. **6**, 22616 (2016). Copyright 2016 Author(s), licensed under a Creative Commons Attribution 4.0 License. (c) is reprinted with permission from Grajower *et al.*, Laser Photonics Rev. **12**, 1700190 (2018). Copyright 2018 Wiley-VCH. (d) is reprinted with permission from Li *et al.*, IEEE Photonics Technol. Lett. **28**, 284 (2016). Copyright 2016 IEEE. (e) is reprinted with permission from Parra *et al.*, Opt. Lett. **44**, 3932 (2019). Copyright 2019 Optical Society of America. (f) is reprinted with permission from Cheung *et al.*, ■ ■, ■ (2023). Copyright 2023 Author(s), licensed under a Creative Commons Attribution 4.0 License.

to the drain. At high source–drain current, electrons gain enough energy to overcome the oxide-silicon energy barrier, and the channel hot electrons are injected into the FG at the drain side. The further electron injection into the top control gate is stopped by the thick blocking dielectric, normally formed by a triple layer of oxide–nitride–oxide. When the bias is removed, the electrons in the floating gate are trapped there. This is called the "Write" operation. To remove the trapped electrons from the FG, the bias polarity at the CG is reversed, forcing the electrons to tunnel back to the p-type Si via Fowler–Nordheim tunneling. This is called the "Erase" operation. If the p-type Si is etched into a waveguide, the same configuration can be used for a non-volatile photonic flash memory. The trapping of electrons inside the FG will modify the effective index of the Si waveguide via free carrier dispersion in a non-volatile way. The concept was first proposed by Barrios and Lipson, where a microring resonator is used to achieve a large modulation depth (91%)[20] [see Fig. 7(a)].

APPLICATIONS OF FLASH MEMORY IN PROGRAMMABLE PHOTONICS

The first silicon photonic flash memory consists of a poly-Si control gate and a Si_3N_4 floating gate embedded in a SiO_2 matrix. SiO_2 acts both as a blocking and tunneling dielectric [Fig. 1(a)].[20] The NPN junction is defined in the partially etched Si waveguide. The experimental demonstration of a silicon photonic flash memory was first reported by Song *et al.,* where they achieved reversible and non-volatile switching of microring resonance[21,90] [see Figs. 1(c) and 7(b)]. The change in both the resonance wavelength and the resonance Q factor indicates that non-volatile switching is indeed caused by the free carrier dispersion of the charges stored in the FG. Multilevel operation is possible by varying the pulse width from 0 to 625 ms with a maximum resonance shift of 380 pm. Finally, a 4-bit memory was demonstrated by controlling four microrings of different radii coupling to a bus waveguide and reading at four different wavelengths. A slightly different configuration was demonstrated by Grajower *et al.* with a Si_3N_4 FG[86] [Fig. 7(c)]. Instead of electrically writing the memory cell, the carriers are injected into the FG via optical excitation (UV illumination), leading to a resonance shift of 125 pm. The thick poly-Si or Si_3N_4 used for FG tends to have minor overlap with the optical mode, which leads to a small effective index change. It is shown that graphene can give a larger effective index change per unit of trapped charges compared to poly-Si[87] [Fig. 7(d)]. Depending on the stored charge density, the optical switch can operate either as an intensity switch or a phase shifter with low insertion loss in the Pauli blocking regime.[91] ITO can also be used for the FG due to its low loss and high conductivity,[88] but in reality, the loss of ITO does vary significantly with its carrier concentration [Fig. 7(e)]. Notably, ITO can be doped by the trapped carriers into the epsilon-near-zero regime, where a large extinction ratio over 10 dB can be realized for a 5 μm long electro-absorption switch. To improve the modulation depth, one can also design the waveguide such that the light is mainly confined in the poly-Si and the FG, which maximizes the overlap between the optical field maxima and the trapped charges.[92] HfO_2 is used as the FG due to its high trap density. A III–V-on-Si photonic flash memory was reported recently in a Mach–Zehnder interferometer, which can be switched reversibly for 100 cycles at <20 pW power consumption.[89]

FERROELECTRIC MATERIALS AND FERROELECTRIC FIELD EFFECT TRANSISTOR

Ferroelectric materials exhibit nonzero spontaneous polarization even when the applied electric field is zero. The polarization can also be reversed by applying a strong enough electric field in the opposite direction. The ability to maintain polarization after the electric field is removed makes them ideal for memory applications. The first application of ferroelectric materials for storage is in FeRAM using lead zirconate titanate (PZT) or strontium bismuth tantalate (SBT), later commercialized by companies such as Samsung and Sony.[93] Traditional FeRAM cell consists of a ferroelectric capacitor connected to the drain of a MOSFET.[16,93] Connecting the capacitor in series with the transistor means that reading the cell will inevitably lead to bit erasure. The discovery of ferroelectricity in Si-doped HfO_2 in 2011 has revived interest in FeFET to realize a highly scalable non-volatile memory.[94] This is because HfO_2 is a more CMOS compatible material, which has been widely used as a gate dielectric, than the traditional perovskite-based materials such as PZT, which are challenging to integrate with the CMOS process. Additionally, since the ferroelectric material now acts as the gate dielectric, the read-out can be non-destructive. The MOSFET-like configuration means the FeFET has both memory and logic functions, so it can be used for in-memory computing or artificial neurons for spiking neural networks.[94] Figure 8 shows the operating principle of a FeFET. The interfacial layer is a thin dielectric, such as SiO_2 or Si_3N_4, that prevents charge leakage and the diffusion of Si into the ferroelectric, which can degrade its properties.[95] The FeFET is written into the ON state (polarization down) when the gate voltage is larger than the positive coercive voltage V_c, which is the bias required to eliminate the macroscopic polarization of the ferroelectrics. This will lead to the accumulation of electrons underneath the gate dielectric, and the drain-source current will increase. On the other hand, the FeFET can be erased by applying an opposite gate voltage that is larger than the negative V_c. This brings the FeFET into the OFF state (polarization up), and electrons in the channel are depleted, causing the drain-source current to drop. As the switching is solely a field driven effect from a low program voltage (typically <5V), FeFET is expected to be a highly energy efficient memory.

APPLICATIONS OF FERROELECTRIC MEMORY IN PROGRAMMABLE PHOTONICS

Although ferroelectric materials have long been explored in photonics, their applications were limited to high-speed modulators, which leveraged the strong Pockels effect of ferroelectric materials such as PZT[96] and Barium Titanate (BTO).[97] The non-volatile effect of ferroelectric in photonics has not been studied until recently, when a silicon photonic phase shifter based on BTO was reported[34] (see Fig. 9). Like a FeFET, the polarization of the ferroelectric BTO layer underneath the silicon can be switched using electrical pulses of different amplitudes or pulse widths, and the bias polarity will determine the polarization orientation. Depending on the orientation of the ferroelectric domains, the Pockel's coefficient changes in a non-volatile fashion, which in turn leads to a refractive index change if the phase shifter is read with a fixed DC voltage bias. Since the ferroelectric switching is entirely based on a field effect, the switching energy can be very low (4.6 pJ). Meanwhile, the use of Pockel's effect
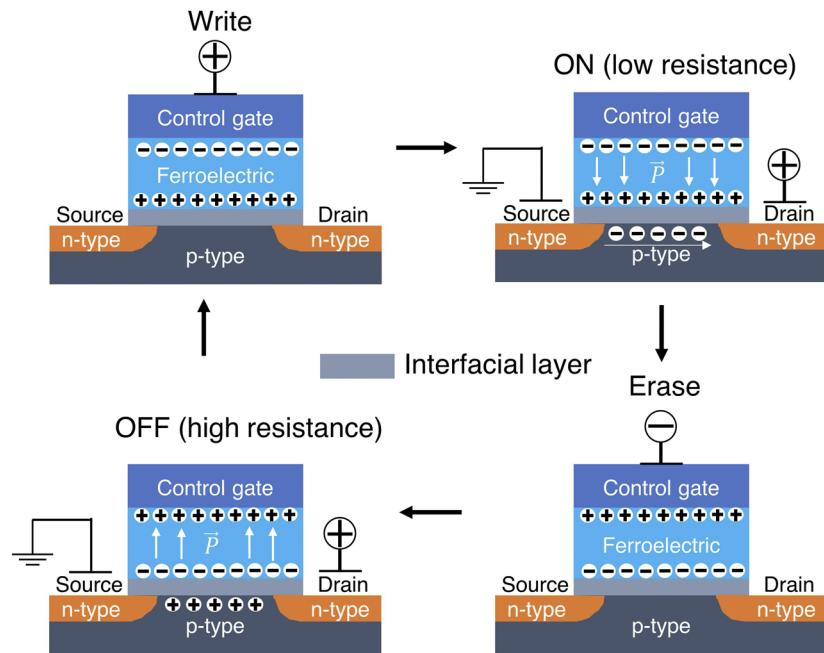
FIG. 8. Operating principle of a FeFET. A FeFET has a similar structure to a MOSFET, where the gate dielectric is replaced with a ferroelectric material. Switching is achieved by applying a bias to the gate, which induces non-volatile polarization of the ferroelectric. The polarization orientation depends on the polarity of the bias. The remanent polarization either causes accumulation or depletion of the carriers in the channel underneath. $\vec{P}$ is the ferroelectric polarization. For applications in programmable photonics, the change in ferroelectric polarization will correspond to a change in the Pockels coefficient of the ferroelectric materials. Hence, if the p-type silicon is etched into a waveguide and a bias is applied across the ferroelectric materials, the effective index of the waveguide mode will be changed in a non-volatile way due to the Pockels effect.

instead of material phase transition or free carrier effect leads to an ultra-low loss of 0.07 dB, which is attractive for photonic quantum computing, which requires very low loss. A highly reliable 8-level operation was also demonstrated. Compared to the other technologies, the main drawback of the ferroelectric phase shifter is that only the change in Pockels coefficient is non-volatile, not the refractive index change, which necessitates a constant bias to read the optical state of the phase shifter. A leakage current of ~200 nA is reported in the recent work, leading to 384 nW of static power in the ON state.[34] Second, Pockel's effect is weaker than PCMs or the free carrier effect, leading to a long L_π of 1 mm. In addition, the low Curie temperature (~120 °C)[98] of BTO may cause erasure of the memory during device thermal cycling. Finally, the hysteretic behavior of ferroelectric materials means that any polarization state will depend on the previous state. Therefore, in order to reliably reach a certain phase shift, the BTO has to be initialized using a long sequence of pulses (~1 ms in total) to restore all the ferroelectric domains to the same polarization.

FERROMAGNETIC MATERIALS AND MAGNETORESISTIVE MEMORY

Ferromagnetic materials such as CoFeB have also been used in random access memory due to their non-volatile and switchable magnetization under magnetic fields.[99] A typical magnetoresistive random access memory (MRAM) cell is made up of a magnetic

tunnel junction (MTJ) connected to a transistor[17] [see Fig. 10]. A MTJ is a tri-layer structure consisting of a free layer, a tunnel barrier, and a reference layer. The free layer is the switchable ferromagnetic layer, typically made of CoFeB alloys with varying compositions, that stores the information. The tunnel barrier is a thin nonmagnetic dielectric, for example, MgO or AlOx, that provides a means to switch and read the state of the free layer. The reference layer does not switch during memory operations and is used to provide a reference frame for the free layer magnetization. The electrons of a certain spin orientation (i.e., spin up or spin down) can tunnel across the barrier only if there are empty states of the same spin orientation available across the junction. Therefore, when the magnetization directions of the free and reference layers are parallel, the majority spin electrons (spin up) will fill the free majority states across the junction, and the minority spin electrons (spin down) will fill the free minority states [see Figs. 10(a) and 10(b)]. This will lead to a larger change in tunneling and, hence, lower resistance. On the other hand, when the magnetization orientations are anti-parallel, the majority of spin electrons on one side will try to fill the minority spin states on the other side, resulting in poor band matching and high resistance [see Fig. 10(b)]. It becomes clear that by switching the magnetization orientation in the free layer, we can switch the resistance of the MTJ, which is typically realized using two approaches shown in Figs. 10(c) and 10(d). A conventional MRAM cell is normally based on the structure shown in Fig. 10(c), where the free layer magnetic switching is induced by the magnetic field generated by the
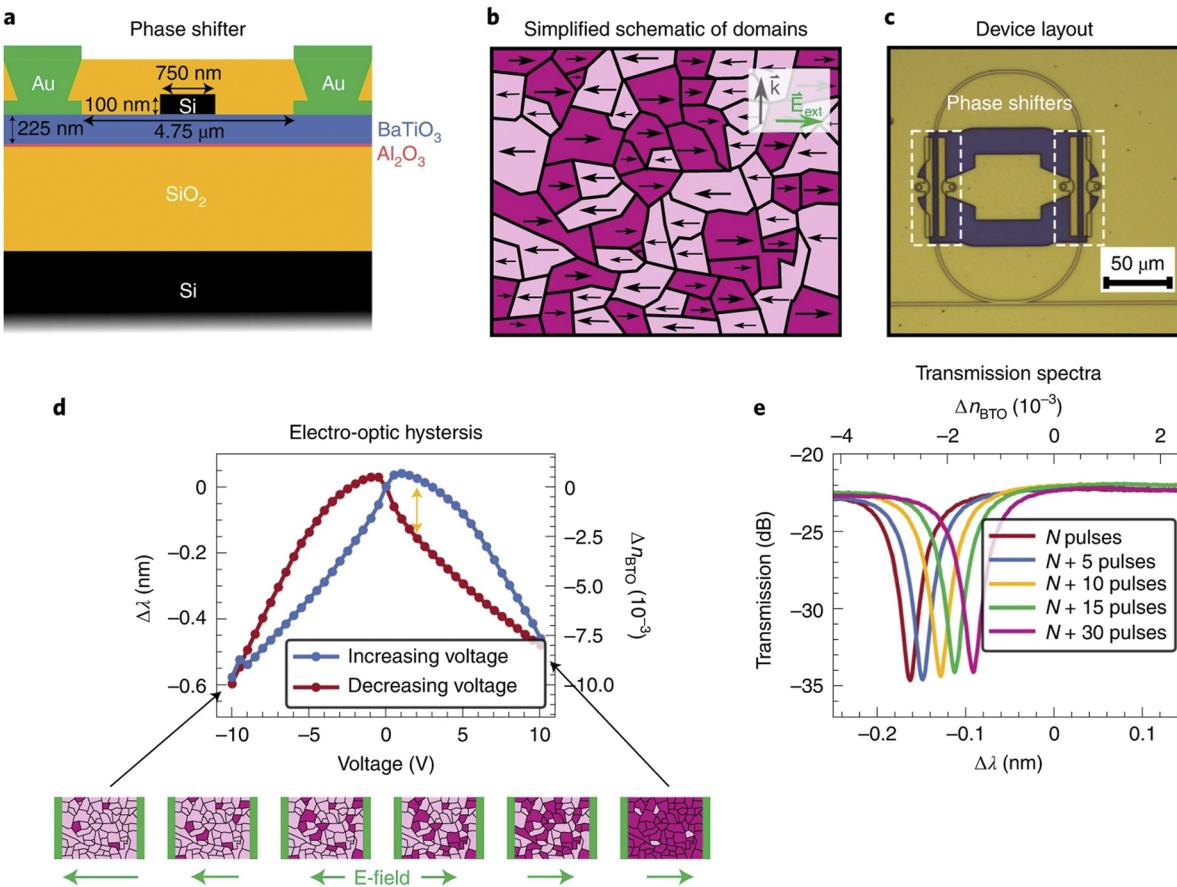
FIG. 9. A non-volatile ferroelectric phase shifter based on BTO. By switching the ferroelectric domain with a sequence of voltage pulses, the Pockels coefficient of the BTO can be changed in a non-volatile way. Under a constant 2V read bias, different phase shifts can be induced due to the Pockels effect, and hence, the microring resonance can be shifted depending on the number of applied pulses. The figure is reprinted with permission from Geler-Kremer *et al.*, Nat. Photonics **16**, 491 (2022). Copyright 2022 Springer Nature.

current injected into the bit and word lines. The switching will only occur when the current passes through both the word and bit lines. The advantage of such an approach is the high switching endurance because the switching is induced solely by a field effect with no physical change in the material structures, as in PCMs and memristors. However, this approach will lead to huge power consumption from the current required to induce the magnetic field, and the fabrication is complicated. Additionally, the magnetic field can also lead to crosstalk, which can accidently switch a nearby cell. To address the limitations, the field has moved toward the spin-transfer-torque MRAM (STT-MRAM) [see Fig. 10(d)]. The magnetization of the free layer can be switched by directly passing current through the MJT, and the magnetization orientation is determined by the polarity of the current and the reference layer.[100] This method eliminates the need for a word line and the crosstalk issue, as only the cell where the current passes will be switched. Most importantly, as the cell width scales down, the write current becomes significantly smaller compared to the traditional MRAM.

APPLICATIONS OF MAGNETORESISTIVE MEMORY IN PROGRAMMABLE PHOTONICS

To convert the MRAM into a photonic MRAM, one simply needs to add a magneto-optic (MO) material into the structure of an MRAM cell such that the magnetization switching induces an optical phase shift. This was first demonstrated by Murai *et al.,* who used the ferromagnetic material CoFeB as an integrated tunable magnet and Ce:YIG as the MO layer to induce a non-volatile phase shift in an a-Si waveguide[33] (see Fig. 11). Passing current through the Cr/Au wire will induce a magnetic field, which switches the magnetization orientation of the CoFeB thin film underneath depending on the current polarity. The CoFeB in turn induces a non-volatile magnetic field onto the Ce:YIG MO layer underneath the a-Si waveguide, which causes a refractive index change. Figure 11(b) shows that such a non-volatile MO phase shifter is integrated into a microring resonator, which produces a 0.14 nm resonance shift after passing two opposite polarities of current at 500 mA through the coil.
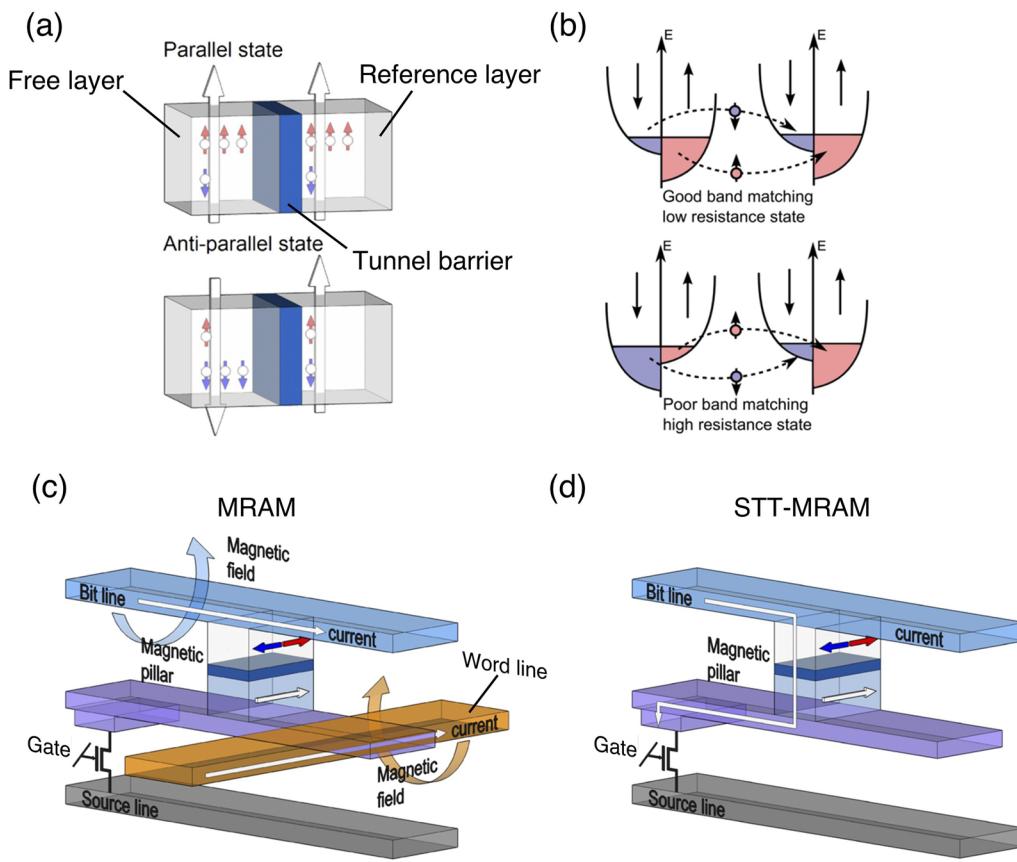
FIG. 10. Operation principle of magnetoresistive random access memory. (a) A magnetic tunnel junction (MTJ) in either parallel or anti-parallel magnetization states. (b) Band diagrams of the MTJ in parallel and anti-parallel states. (c) Schematic of a conventional MRAM cell. The magnetic pillar corresponds to the MTJ shown in (a). (d) Schematic of a STT-MRAM. Figures (a) to (d) are reprinted with permission from A. Makarov, ■ dissertation (■, ■).[101]

A 2 by 2 Mach–Zehnder interferometer switch was also demonstrated with an extinction ratio of 25 dB. Although endurance is not reported in the paper, high endurance is expected because the magneto-switching does not involve any structural change of the materials. Second, the phase shifter can be driven by low voltages (±0.5 V) at the cost of a large device footprint (1.2 mm). However, the high-power consumption (250 mW) for switching is a clear disadvantage compared to other technologies such as memristors and ferroelectrics. Additionally, the MO effect is weak due to the large spacing between the CoFeB and the MO layer, resulting in a long L_π of 1.2 mm. The reported insertion loss (~10 dB) of the MZI switch is also prohibitive for large-scale systems.

OPTICAL MEMORY BASED ON VO₂

Similar to PCMs, VO_2 is another class of phase-transition materials that can be reversibly switched between an insulator and metallic phase via electrical, optical, and thermal excitations ($T_c \sim 70\,^\circ$C).[102] Due to the enormous change in the refractive index (Δn, $\Delta k > 2$ *near* 1550 nm), VO_2 is widely used in programmable photonics with applications ranging from electro-absorptive

silicon photonic switches[103] to tunable metasurfaces.[104] Despite these advantages, the phase transition of VO_2 is volatile—once the excitation is removed, the material will return to the insulator phase. It was only recently that people discovered a way to realize an optical memory in VO_2[35] on a silicon photonic waveguide. The optical memory consists of VO_2 cladded on top of a Si waveguide contacted by electrodes (see Fig. 12). Under electrical bias, a hysteresis loop is observed in the I–V curve due to the insulator-metal-transition (IMT), where the current suddenly increases at threshold voltage. However, once the bias is removed, the VO_2 returns to the high resistance state as the hysteretic behavior is volatile. To write the memory, optical pulses are used to trigger the IMT while the bias is held near the threshold voltage. If the bias is maintained, VO_2 will stay in the metallic state with high absorption. To erase the memory, the bias is turned off, and the VO_2 returns to the insulator phase. The memory can be read either optically through the waveguide transmission or electrically through the resistance. In this way, a light pulse triggered volatile optical memory is realized. Although the switching energy is very low (~23.5 pJ), substantial power is consumed by holding the memory cell at a high bias voltage (~13 mW).

(a)

(b)
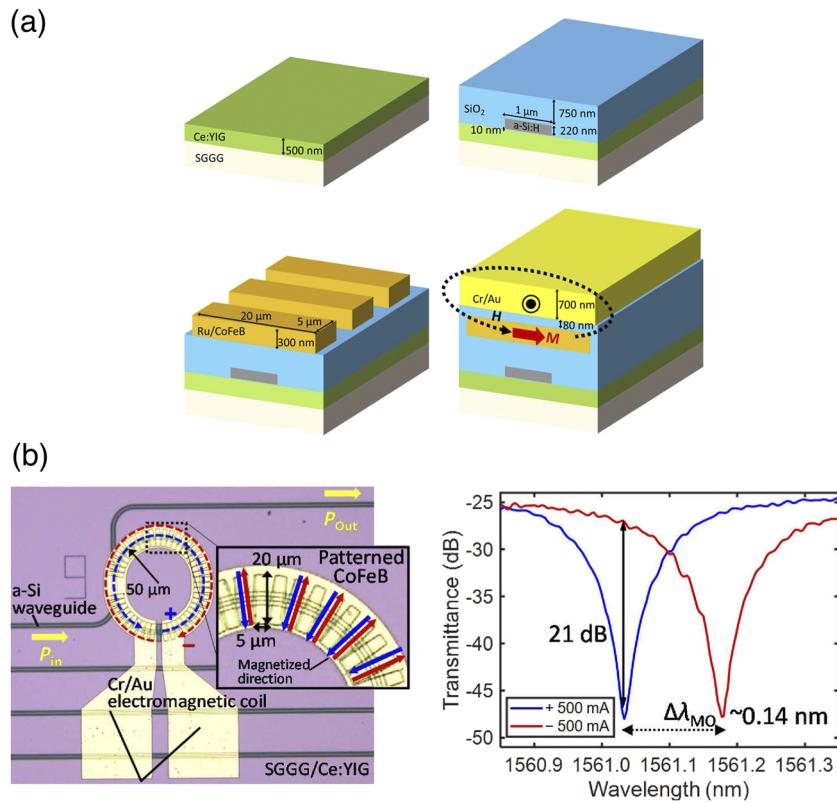
FIG. 11. A non-volatile magneto-optic phase shifter. (a) Schematic showing the structure of the magneto-optic phase shifter. The magnetization of the CoFeB can be switched by passing current through Cr/Au electrodes. Ce-YIG is a magneto-optic material whose refractive index changes in response to the magnetic field induced by CoFeB. (b) A microring integrated with the magneto-optic phase shifter. A non-volatile magneto-optic wavelength shift of 0.14 nm can be induced by passing 500 mA current through the electrodes. The figures are reprinted with permission from Murai *et al.*, Opt. Express **28**, 31675 (2020). Copyright 2020 Optical Society of America.

COMPARISON BETWEEN DIFFERENT NON-VOLATILE PHOTONIC TECHNOLOGIES

After reviewing these different non-volatile materials, we compare their pros and cons in Table I. We see that the biggest advantage of PCMs is their compact footprint, requiring only tens of micrometers to attain π phase shift, compared to hundreds of micrometers using other technologies under the same bias level or electric field strength. Second, they are a truly "set-and-forget" technology that does not require any external bias or power to maintain their states. This allows the PCM-based devices to be unplugged from the power source in a static state. On the other hand, insertion loss has been the main limitation of PCMs due to the constraint of Kramer–König relations, which stipulates an increase in loss whenever there is an increase in the real part of the refractive index. Even with the discovery of low-loss PCMs,[48,49] it is still challenging to reduce the loss below 0.1 dB/π. The switching time of PCMs is also relatively slow in photonics, which prevents them from high-speed operation. Overall, we think PCMs are well-suited for applications that only require infrequent reconfiguration, and the switches mainly stay in the static state, such as photonic RAM, trimming photonic resonators, optical routing in PICs, and inference for optical neural networks.

Both flash memory and ferroelectric memory are based on the field effect for reconfiguration, which explains why they have very similar switching speed, energy, and modulation strength. The key difference is that flash memory can be truly "set-and-forget," while ferroelectric memory will require a constant read bias to trigger the EO effect. In addition, flash memory is also more CMOS compatible than ferroelectric materials, which are not supported in most commercial foundries. However, ferroelectric materials induce very low insertion loss compared to the high insertion loss caused by the free carrier absorption in photonic flash memory. Flash memory also tends to require a relatively high driving voltage (>10V) to force the tunneling of charges, while ferroelectric materials can typically be switched at <5V.[93] Another drawback of flash memory is its sensitivity to high energy radiation,[86] which can limit its applications in extreme environments such as aerospace. Finally, flash memory tends to have lower switching speeds in the range of a few hundred microseconds.[21] We think flash memory will be well-suited for applications where loss and speed are not critical and the information must be stored in a non-volatile way, for example, photonic RAM, but exposure to UV radiation should be avoided. In contrast, ferroelectric memory will have advantages in quantum PICs where loss is critical,[2] thanks to its wide bandgap and the ability to operate
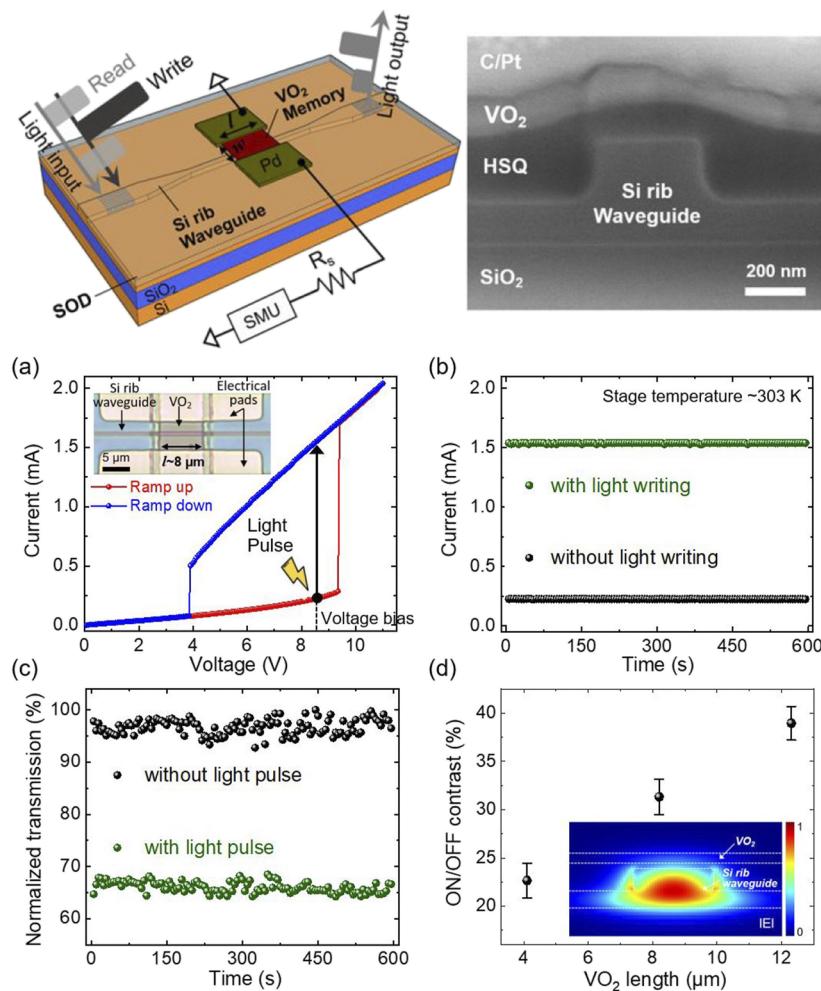
FIG. 12. Optical memory based on VO$_2$. When the memory cell is held at a constant bias of 9 V in the high transmission and resistance state, it can be switched into the low transmission and resistance state by a 100 ns optical pulse. The cell can be returned to its high transmission and resistance state by removing the voltage bias. The optical contrast can be increased by using a longer VO$_2$ segment. The figure is reprinted with permission from Jung *et al.*, ACS Photonics **9**, 217 (2022). Copyright 2022 Author(s), licensed under a Creative Commons Attribution 4.0 License.

at cryogenic temperatures.[109] One exception is ferromagnetic memory, which is based on the field effect[33] yet consumes large amounts of power (~250 mW). A non-volatile MO phase shifter based on ferromagnetic materials will be ideal for applications that require very high endurance and truly "set-and-forget" operation at low voltages (±0.5V), but the large power consumption and insertion loss will be crucial problems that need to be solved before it can be scaled up.

In terms of memristors, they can provide the highest speed and the lowest switching energy because only nanoscale filaments are switched. Similar to flash memory, they are highly CMOS compatible, as the active layer can simply be dielectrics such as SiO$_2$, Al$_2$O$_3$, or HfO$_2$. However, depending on their configuration (plasmonics or photonics), they will have very different performance metrics. Plasmonic memristors can be "set-and-forget" but are very lossy, which

limits their application to a single standalone device, such as photon sources[32] or detectors.[82] The high loss will also be prohibitive for phase shifters. On the other hand, photonic memristors can be a scalable technology thanks to their lower loss and CMOS compatibility, but they require a constant bias to read the optical state, similar to ferroelectric materials. Such DC power consumption is much smaller than VO$_2$ but still non-negligible (~nW to μW), especially when the memristor is in the low resistance state. We think they can be potentially used for photonic in-memory computing, where the weight of the neuron can be updated at high speeds during training. Another application is a spatial light modulator where each pixel in a 2D array can be tuned by a memristor at high speed, while the 2D phase mask can be maintained by applying a constant bias to all the pixels. Finally, although VO$_2$ optical memory exhibits large switching contrasts and can be tuned at relatively high speed

TABLE I. For PCMs, the first number quoted is for crystallization, and the second number is for amorphization. For memristors and flash memory, the first number quoted is for SET, and the second number is for RESET. The L_π is not quoted for GST, GSST, plasmonic memristors, and VO_2 because the high insertion loss prohibits phase-only modulation. ✓ means yes, × means no, and ○ means questionable. In the column "Non-volatile?," ○ means not "set-and-forget," i.e., a bias is required to read the optical memory state. "Amp." is short for amplitude. "Sim." is short for simulation.

Technology	Materials	Amp. Or phase?	Insertion loss (dB)	Switching time (μs)	Switching energy(nJ)	$L_\pi(\mu m)$	Endurance	Electrical control?	Non-volatile?	CMOS compatible?
PCMs[23,105]	GST	Amp.	1.6	15/0.025	17/0.18	⋯	1000	×	✓	○
PCMs[51]	GST	Amp.	0.9/0.2	160/0.1	78/8	⋯	500	✓	✓	○
PCMs[47]	GSST	Amp.	<0.5	10^5/0.1	4.25×10^7/5500	⋯	1000	×	✓	○
PCMs[56]	Sb_2Se_3	Phase	0.5	5×10^4/0.4	9.5×10^5/14	25	600	×	✓	○
PCMs[106]	Sb_2Se_3	Phase	0.36	1000/0.8	3.8×10^7/1.8×10^5	11	125	✓	✓	○
PCMs[60]	Sb_2Se_3	Phase	0.33	220/0.4	63/0.38	430	1000	✓	✓	○
PCMs[107]	Sb_2S_3	Phase	0.48	10^6/0.2	1.3×10^6/90	47	1	✓	✓	○
PCMs[108]	Sb_2S_3	Phase	0.72	100/0.15	1.7×10^3/56	30.7	800	✓	✓	○
Flash memory[21]	Poly-Si	Amp.	2–14.7	6×10^5/2.25×10^5	0.017/0.011	981	30	✓	✓	✓
Flash memory[89]	Al_2O_3 and HfO_2	Phase	0.175 (sim.)	⋯	⋯	2500	100	✓	✓	✓
Ferroelectric[34]	BTO	Phase	0.07	1000	4.6–26.7×10^{-3}	1000	⋯	✓	○	○
Memristor[77]	SiO_2	Amp.	5/10	0.033	10 μJ/1 nJ	⋯	⋯	✓	✓	✓
Memristor[31]	HfO_2	Phase	0.28	0.1	1.3×10^{-3}/4×10^{-4}	534	800	✓	○	✓
Memristor[30]	Al_2O_3	Phase	0.05	3×10^{-4}/9×10^{-4}	1.5×10^{-4}/3.6×10^{-4}	349	1000	✓	○	✓
Ferromagnetic	CoFeB	Phase	10	1	100	1200	⋯	✓	✓	○
VO_2[35]	VO_2	Amp.	3.8	0.1	0.0235	⋯	10000	✓	×	○

26 October 2023 02:57:41

with low switching energy, the absence of non-volatility is a major limitation as ~mW of power is consumed to maintain the state. The large insertion loss and high-power consumption make VO_2 a less competitive candidate for non-volatile programmable photonics compared to other technologies.

OUTLOOK

In this section, we discuss challenges that need to be addressed to advance the field and identify future research directions. Different materials will be discussed individually in separate sub-sections.

Phase-change materials

Phase-change materials can play an important role in applications that only require infrequent switching, such as photonic RAM, trimming photonic resonators, optical routing in PICs, and inference for optical neural networks. To further scale up the technology, two crucial bottlenecks must be overcome. First, current photonic devices based on PCMs still suffer from relatively high insertion loss (>1 dB). The loss must be reduced below 0.01 dB per device to be useful in large-scale PICs, which will require either careful device engineering[110] and/or very low-loss PCMs with bandgap energy in the ultraviolet range.[111] Second, no commercial silicon photonics foundry has supported PCMs so far. Foundries must be willing to incorporate PCMs into their processes so that they can be produced on a wafer scale. This will require first showing attractive functionalities or improved performance from large-scale integrated systems in industrial or academic research settings, which can draw substantial and long-term investment interest. A short-term solution is to deposit PCMs in a back-end-of-the-line process on foundry fabricated wafers,[106] but opening windows in the oxide cladding near active devices for PCM deposition can be a challenging task at the wafer scale.[112]

Flash memory

Flash memory is a technology that can be easily scaled up with the current CMOS process. Particularly, photonic flash memory may be the best approach to realize non-volatile photonic RAM, which harnesses the mature flash memory technology developed in the electronic industry. However, current photonic flash memory still relies on carrier injection for modulation, so it will not be ideal for low-loss components such as phase shifters, whereas the driving voltage remains high (20V) and the speed is slow (a few hundred microseconds). While the high insertion loss can be difficult to circumvent due to the nature of carrier dispersion, many studies have proposed different materials and geometry for photonic flash memory that can solve the high driving voltage issue, for example, by guiding the light directly in the charge trapping layers[92] or using graphene as the floating gate.[87] We expect to see experimental demonstrations of these ideas as more researchers start to work in this field.

Memristors

Memristor is a promising non-volatile technology that can enable fast and energy-efficient switching and, hence, have potential applications in in-memory optical computing and high-speed spatial light modulation. Similar to flash memory, it is also entirely based on CMOS compatible materials. We believe photonic memristors will be a more promising solution for scalability compared to plasmonic memristors, but a few limitations must be addressed before they can be a competitive technology. More specifically, the DC power required to read the optical state (~nW to μW)—particularly in the low resistance state—is much higher than that of ferroelectrics and other technologies that do not require a read bias. To mitigate this, the device can be read using short voltage pulses. In this way, the device does not require a constant voltage bias, and read/write voltage is only applied during read and write cycles. In the case of inference for neural networks, for example, it only needs to be written once and then read whenever the vector-matrix-multiplication is being performed. Second, the insertion loss is still relatively high as it is based on carrier effects. One potential solution is to connect the memristor in series with a phase shifter based on EO materials such as BTO or lithium niobate. A constant bias is applied to the EO phase shifter, while the memristor will act as a non-volatile switch to turn the EO effect on and off. This is possible because the resistance of the memristor will determine how much voltage is dropped on the EO phase shifter and on the memristor. The resistance contrast between the LRS and HRS can be larger than 1000 times. Meanwhile, applying a constant bias to the EO phase shifter will consume minimal power due to the low current leakage. In this way, the advantages of both ferroelectrics and memristors can be combined to enable a fast and non-volatile photonic phase shifter with low loss and near zero static power consumption.

Ferroelectric materials

Two key advantages of ferroelectric materials over other technologies are their very low loss and switching energy. The low loss comes from the fact that the reconfiguration mechanism is based on the EO effect rather than the carrier dispersion effect, while the low switching energy can be attributed to field-induced ferroelectric domain switching instead of current-driven switching. On the other hand, two main challenges need to be overcome before wider adoption of this technology. First, the current BTO ferroelectric materials have poor CMOS compatibility, which has to be grown epitaxially and then transferred to a substrate through wafer bonding.[97] Although companies like Intel have already successfully introduced heterogeneous integration into their silicon photonics process, a larger incentive, for example, the potential of using BTO as a Pockels material, is still needed to convince the foundries that it is worth the investment to introduce BTO into the fab line. A recent study has shown that the ferroelectric material Hafnium zirconium oxide (HZO), which is a CMOS compatible material and can be easily deposited via sputtering, exhibits a non-volatile phase shifting effect.[113] However, the reversible phase transition and the material's Pockels effect were not reported, while the switching voltage is prohibitively high (210 V). Second, the ferroelectric phase shifter still requires a bias to read the optical state, which can complicate the CMOS control as the switching and read pulses need to be synchronized and temporally separated. A potential future research direction will be to investigate whether ferroelectric domain switching can lead to a refractive index change by itself without requiring read bias.

26 October 2023 02:57:41

Ferromagnetic materials

One unique advantage of ferromagnetic materials is their potentially high endurance, as magnetic switching does not involve any material's structural changes. Unfortunately, no literature has shown this ultra-high endurance in experiments. Experimental verification of this high endurance in ferromagnetic materials can have a high impact on the non-volatile photonics research field. The main drawback of ferromagnetic phase shifters is the high switching power (250 mW) and weak optical phase shift due to (1) the large spacing between the CoFeB and the Ce:YIG where the waveguide lies and (2) the small mode overlap between the silicon waveguide and the Ce:YIG. To increase the mode overlap with the MO material, we can leverage the mature Si_3N_4 platforms, which have a lower index contrast compared to Si and have been shown to have a higher MO figure of merit.[114] Meanwhile, instead of placing Ce:YIG beneath the waveguide, one can bond Ce:YIG directly on top of the waveguide.[115] By doing this, the CoFeB can then be brought into contact with the MO materials, as the Ce:YIG itself can act as a spacer between the absorptive CoFeB and the optical mode, and the CoFeB can exert a much stronger magnetic field onto the Ce:YIG.

In summary, we have reviewed the recent development of non-volatile materials for programmable photonics applications. These include phase-change materials, flash memory, ferroelectric materials, ferromagnetic materials, memristors, and VO_2. We briefly explain the working principles behind these materials and discuss their applications in non-volatile photonics. We compare the advantages and disadvantages of different technologies and identify their target applications. Finally, we discuss the crucial challenges and point out potential future research directions to advance the field.

AUTHOR DECLARATIONS

Conflict of Interest

The authors have no conflicts to disclose.

Author Contributions

Zhuoran Fang: Writing – original draft (lead). **Rui Chen**: Writing – review & editing (equal). **Bassem Tossoun**: Writing – review & editing (equal). **Stanley Cheung**: Writing – review & editing (equal). **Di Liang**: Writing – review & editing (equal). **Arka Majumdar**: Writing – review & editing (equal).

DATA AVAILABILITY

The data that support the findings of this study are available from the corresponding author upon reasonable request.

REFERENCES

[1] Y. Shen, N. C. Harris, S. Skirlo, M. Prabhu, T. Baehr-Jones, M. Hochberg, X. Sun, S. Zhao, H. Larochelle, D. Englund, and M. Soljačić, "Deep learning with coherent nanophotonic circuits," Nat. Photonics **11**(7), 441–446 (2017).

[2] J. M. Arrazola, V. Bergholm, K. Brádler, T. R. Bromley, M. J. Collins, I. Dhand, A. Fumagalli, T. Gerrits, A. Goussev, L. G. Helt, J. Hundal, T. Isacsson, R. B. Israel, J. Izaac, S. Jahangiri, R. Janik, N. Killoran, S. P. Kumar, J. Lavoie, A. E. Lita, D. H. Mahler, M. Menotti, B. Morrison, S. W. Nam, L. Neuhaus, H. Y. Qi, N. Quesada, A. Repingon, K. K. Sabapathy, M. Schuld, D. Su, J. Swinarton, A. Száva, K. Tan, P. Tan, V. D. Vaidya, Z. Vernon, Z. Zabaneh, and Y. Zhang, "Quantum circuits with many photons on a programmable nanophotonic chip," Nature **591**(7848), 54–60 (2021).

[3] M. R. Watts, J. Sun, C. DeRose, D. C. Trotter, R. W. Young, and G. N. Nielson, "Adiabatic thermo-optic Mach–Zehnder switch," Opt. Lett. **38**(5), 733–735 (2013).

[4] W. M. J. Green, M. J. Rooks, L. Sekaric, and Y. A. Vlasov, "Ultra-compact, low RF power, 10 Gb/s silicon Mach-Zehnder modulator," Opt. Express **15**(25), 17106–17113 (2007).

[5] M. He, M. Xu, Y. Ren, J. Jian, Z. Ruan, Y. Xu, S. Gao, S. Sun, X. Wen, L. Zhou, L. Liu, C. Guo, H. Chen, S. Yu, L. Liu, and X. Cai, "High-performance hybrid silicon and lithium niobate Mach–Zehnder modulators for 100 Gbit s^{-1} and beyond," Nat. Photonics **13**(5), 359–364 (2019).

[6] C. Errando-Herranz, A. Y. Takabayashi, P. Edinger, H. Sattari, K. B. Gylfason, and N. Quack, "MEMS for photonic integrated circuits," IEEE J. Sel. Top. Quantum Electron. **26**(2), 8200916 (2020).

[7] S. Y. Siew, B. Li, F. Gao, H. Y. Zheng, W. Zhang, P. Guo, S. W. Xie, A. Song, B. Dong, L. W. Luo, C. Li, X. Luo, and G.-Q. Lo, "Review of silicon photonics technology and platform development," J. Lightwave Technol. **39**(13), 4374–4389 (2021).

[8] Q. Cheng, S. Rumley, M. Bahadori, and K. Bergman, "Photonic switching in high performance datacenters (Invited)," Opt. Express **26**(12), 16022–16043 (2018).

[9] N. K. Fontaine, R. Ryf, H. Chen, D. T. Neilson, K. Kim, and J. Carpenter, "Laguerre-Gaussian mode sorter," Nat. Commun. **10**(1), 1865 (2019).

[10] P. Hosseini, C. D. Wright, and H. Bhaskaran, "An optoelectronic framework enabled by low-dimensional phase-change films," Nature **511**(7508), 206–211 (2014).

[11] A. H. Atabaki, A. A. Eftekhar, M. Askari, and A. Adibi, "Accurate post-fabrication trimming of ultra-compact resonators on silicon," Opt. Express **21**(12), 14139–14145 (2013).

[12] H. Jayatilleka, H. Frish, R. Kumar, J. Heck, C. Ma, M. N. Sakib, D. Huang, and H. Rong, "Post-fabrication trimming of silicon photonic ring resonators at wafer-scale," J. Lightwave Technol. **39**(15), 5083–5088 (2021).

[13] M. Wuttig and N. Yamada, "Phase-change materials for rewriteable data storage," Nat. Mater. **6**(11), 824–832 (2007).

[14] G. W. Burr, M. J. Breitwisch, M. Franceschini, D. Garetto, K. Gopalakrishnan, B. Jackson, B. Kurdi, C. Lam, L. A. Lastras, A. Padilla, B. Rajendran, S. Raoux, and R. S. Shenoy, "Phase change memory technology," J. Vac. Sci. Technol. B **28**(2), 223–262 (2010).

[15] F. Pan, S. Gao, C. Chen, C. Song, and F. Zeng, "Recent progress in resistive random access memories: Materials, switching mechanisms, and performance," Mater. Sci. Eng., R **83**, 1–59 (2014).

[16] T. Mikolajick, U. Schroeder, and S. Slesazeck, "The past, the present, and the future of ferroelectric memories," IEEE Trans. Electron Devices **67**(4), 1434–1443 (2020).

[17] D. Apalkov, B. Dieny, and J. M. Slaughter, "Magnetoresistive random access memory," Proc. IEEE **104**(10), 1796–1830 (2016).

[18] R. Bez, E. Camerlenghi, A. Modelli, and A. Visconti, "Introduction to flash memory," Proc. IEEE **91**(4), 489–502 (2003).

[19] R. J. Walters, P. G. Kik, J. D. Casperson, H. A. Atwater, R. Lindstedt, M. Giorgi, and G. Bourianoff, "Silicon optical nanocrystal memory," Appl. Phys. Lett. **85**(13), 2622–2624 (2004).

[20] C. A. Barrios and M. Lipson, "Silicon photonic read-only memory," J. Lightwave Technol. **24**(7), 2898 (2006).

26 October 2023 02:57:41

[21] J.-F. Song, X.-S. Luo, A. E.-J. Lim, C. Li, Q. Fang, T.-Y. Liow, L.-X. Jia, X.-G. Tu, Y. Huang, H.-F. Zhou, and G.-Q. Lo, "Integrated photonics with programmable non-volatile memory," Sci. Rep. **6**(1), 22616 (2016).

[22] H. Tsuda, *Asia Communications and Photonics Conference and Exhibition* (IEEE, 2010), pp. 540–541.

[23] C. Ríos, M. Stegmaier, P. Hosseini, D. Wang, T. Scherer, C. D. Wright, H. Bhaskaran, and W. H. P. Pernice, "Integrated all-photonic non-volatile multi-level memory," Nat. Photonics **9**(11), 725–732 (2015).

[24] J. Feldmann, N. Youngblood, M. Karpov, H. Gehring, X. Li, M. Stappers, M. Le Gallo, X. Fu, A. Lukashchuk, A. S. Raja, J. Liu, C. D. Wright, A. Sebastian, T. J. Kippenberg, W. H. P. Pernice, and H. Bhaskaran, "Parallel convolutional processing using an integrated photonic tensor core," Nature **589**(7840), 52–58 (2021).

[25] A. Emboras, I. Goykhman, B. Desiatov, N. Mazurski, L. Stern, J. Shappir, and U. Levy, "Nanoscale plasmonic memristor with optical readout functionality," Nano Lett. **13**(12), 6151–6155 (2013).

[26] B. Tossoun, X. Sheng, J. P. Strachan, and D. Liang, in *2020 IEEE International Electron Devices Meeting (IEDM)* (IEEE, 2020), p. 7.6.1–7.6.4.

[27] B. Tossoun, X. Sheng, J. P. Strachan, D. Liang, and R. G. Beausoleil, in *Photonics in Switching and Computing 2021*, Paper No. Tu5B.3 (Optica Publishing Group, 2021), p. Tu5B.3.

[28] S. Cheung, B. Tossoun, Y. Yuan, Y. Peng, G. Kurczveil, Y. Hu, X. Xian, D. Liang, and R. G. Beausoleil, in *Conference on Lasers and Electro-Optics 2022*, Paper No. STu5G.6 (Optica Publishing Group, 2022), p. STu5G.6.

[29] S. Cheung, B. Tossoun, Z. Fang, Y. Yuan, Y. Hu, G. Kurczveil, Y. Peng, D. Liang, and R. G. Beausoleil, in *2022 IEEE Photonics Conference (IPC)* (IEEE, 2022), pp. 1–2.

[30] B. Tossoun, D. Liang, S. Cheung, Z. Fang, X. Sheng, J. P. Strachan, and R. G. Beausoleil, "High-speed and energy-efficient non-volatile silicon photonic memory based on heterogeneously integrated memresonator," arXiv:2303.05644 (2023).

[31] Z. Fang, B. Tossoun, A. Descos, D. Liang, X. Huang, G. Kurczveil, A. Majumdar, and R. G. Beausoleil, in *Optical Fiber Communication Conference (OFC) 2023*, Paper No. W3G.3 (Optica Publishing Group, 2023), p. W3G.3.

[32] B. Cheng, T. Zellweger, K. Malchow, X. Zhang, M. Lewerenz, E. Passerini, J. Aeschlimann, U. Koch, M. Luisier, A. Emboras, A. Bouhelier, and J. Leuthold, "Atomic scale memristive photon source," Light Sci. Appl. **11**(1), 78 (2022).

[33] T. Murai, Y. Shoji, N. Nishiyama, and T. Mizumoto, "Nonvolatile magneto-optical switches integrated with a magnet stripe array," Opt. Express **28**(21), 31675–31685 (2020).

[34] J. Geler-Kremer, F. Eltes, P. Stark, D. Stark, D. Caimi, H. Siegwart, B. Jan Offrein, J. Fompeyrine, and S. Abel, "A ferroelectric multilevel non-volatile photonic phase shifter," Nat. Photonics **16**(7), 491–497 (2022).

[35] Y. Jung, H. Han, A. Sharma, J. Jeong, S. S. P. Parkin, and J. K. S. Poon, "Integrated hybrid VO_2–silicon optical memory," ACS Photonics **9**(1), 217–223 (2022).

[36] M. T. Hill, H. J. S. Dorren, T. de Vries, X. J. M. Leijtens, J. H. den Besten, B. Smalbrugge, Y.-S. Oei, H. Binsma, G.-D. Khoe, and M. K. Smit, "A fast low-power optical memory based on coupled micro-ring lasers," Nature **432**(7014), 206–209 (2004).

[37] K. Nozaki, A. Shinya, S. Matsuo, Y. Suzaki, T. Segawa, T. Sato, Y. Kawaguchi, R. Takahashi, and M. Notomi, "Ultralow-power all-optical RAM based on nanocavities," Nat. Photonics **6**(4), 248–252 (2012).

[38] L. Liu, R. Kumar, K. Huybrechts, T. Spuesens, G. Roelkens, E.-J. Geluk, T. de Vries, P. Regreny, D. Van Thourhout, R. Baets, and G. Morthier, "An ultra-small, low-power, all-optical flip-flop memory on a silicon chip," Nat. Photonics **4**(3), 182–187 (2010).

[39] E. Kuramochi, K. Nozaki, A. Shinya, K. Takeda, T. Sato, S. Matsuo, H. Taniyama, H. Sumikura, and M. Notomi, "Large-scale integration of wavelength-addressable all-optical memories on a photonic crystal chip," Nat. Photonics **8**(6), 474–481 (2014).

[40] P. Edinger, A. Y. Takabayashi, C. Errando–Herranz, U. Khan, C. Antony, G. Talli, P. Verheyen, W. Bogaerts, N. Quack, and K. B. Gylfason, in *2022 IEEE 35th International Conference on Micro Electro Mechanical Systems Conference (MEMS)* (IEEE, 2022), pp. 995–997.

[41] M. Zhu, O. Cojocaru-Mirédin, A. M. Mio, J. Keutgen, M. Küpers, Y. Yu, J.-Y. Cho, R. Dronskowski, and M. Wuttig, "Unique bond breaking in crystalline phase change materials and the quest for Metavalent bonding," Adv. Mater. **30**(18), 1706735 (2018).

[42] J. Zheng, A. Khanolkar, P. Xu, S. Colburn, S. Deshmukh, J. Myers, J. Frantz, E. Pop, J. Hendrickson, J. Doylend, N. Boechler, and A. Majumdar, "GST-on-silicon hybrid nanophotonic integrated circuits: A non-volatile quasi-continuously reprogrammable platform," Opt. Mater. Express **8**(6), 1551–1561 (2018).

[43] M. Wuttig, H. Bhaskaran, and T. Taubner, "Phase-change materials for non-volatile photonic applications," Nat. Photonics **11**(8), 465–476 (2017).

[44] Z. Fang, R. Chen, J. Zheng, and A. Majumdar, "Non-volatile reconfigurable silicon photonics based on phase-change materials," IEEE J. Sel. Top. Quantum Electron. **28**, 8200317 (2021).

[45] C. Rios, P. Hosseini, C. D. Wright, H. Bhaskaran, and W. H. P. Pernice, "On-chip photonic memory elements employing phase-change materials," Adv. Mater. **26**(9), 1372–1377 (2014).

[46] Z. Fang, R. Chen, V. Tara, and A. Majumdar, "Non-volatile phase-change materials for programmable photonics," Sci. Bull. **68**, 783 (2023).

[47] Y. Zhang, J. B. Chou, J. Li, H. Li, Q. Du, A. Yadav, S. Zhou, M. Y. Shalaginov, Z. Fang, H. Zhong, C. Roberts, P. Robinson, B. Bohlin, C. Ríos, H. Lin, M. Kang, T. Gu, J. Warner, V. Liberman, K. Richardson, and J. Hu, "Broadband transparent optical phase change materials for high-performance nonvolatile photonics," Nat. Commun. **10**(1), 4279 (2019).

[48] M. Delaney, I. Zeimpekis, D. Lawson, D. W. Hewak, and O. L. Muskens, "A new family of ultralow loss reversible phase-change materials for photonic integrated circuits: Sb_2S_3 and Sb_2Se_3," Adv. Funct. Mater. **30**(36), 2002447 (2020).

[49] W. Dong, H. Liu, J. K. Behera, L. Lu, R. J. H. Ng, K. V. Sreekanth, X. Zhou, J. K. W. Yang, and R. E. Simpson, "Wide bandgap phase change material tuned visible photonics," Adv. Funct. Mater. **29**(6), 1806181 (2019).

[50] B. J. Kooi and M. Wuttig, "Chalcogenides by design: Functionality through Metavalent bonding and confinement," Adv. Mater. **32**(21), 1908302 (2020).

[51] J. Zheng, Z. Fang, C. Wu, S. Zhu, P. Xu, J. K. Doylend, S. Deshmukh, E. Pop, S. Dunham, M. Li, and A. Majumdar, "Nonvolatile electrically reconfigurable integrated photonic switch enabled by a silicon PIN diode heater," Adv. Mater. **32**(31), 2001218 (2020).

[52] F. Xiong, A. D. Liao, D. Estrada, and E. Pop, "Low-power switching of phase-change materials with carbon nanotube electrodes," Science **332**(6029), 568–570 (2011).

[53] D. Tanaka, Y. Shoji, M. Kuwahara, X. Wang, K. Kintaka, H. Kawashima, T. Toyosaki, Y. Ikuma, and H. Tsuda, "Ultra-small, self-holding, optical gate switch using $Ge_2Sb_2Te_5$ with a multi-mode Si waveguide," Opt. Express **20**(9), 10283–10294 (2012).

[54] M. Rudé, J. Pello, R. E. Simpson, J. Osmond, G. Roelkens, J. J. G. M. van der Tol, and V. Pruneri, "Optical switching at 1.55 μm in silicon racetrack resonators using phase change materials," Appl. Phys. Lett. **103**(14), 141119 (2013).

[55] C. Wu, H. Yu, H. Li, X. Zhang, I. Takeuchi, and M. Li, "Low-loss integrated photonic switch using subwavelength patterned phase change material," ACS Photonics **6**(1), 87–92 (2019).

[56] M. Delaney, I. Zeimpekis, H. Du, X. Yan, M. Banakar, D. J. Thomson, D. W. Hewak, and O. L. Muskens, "Nonvolatile programmable silicon photonics using an ultralow-loss Sb_2Se_3 phase change material," Sci. Adv. **7**(25), eabg3500 (2021).

[57] R. Chen, Z. Fang, F. Miller, H. Rarick, J. E. Fröch, and A. Majumdar, "Opportunities and challenges for large-scale phase-change material integrated electro-photonics," ACS Photonics **9**(10), 3181–3195 (2022).

[58] K. Kato, M. Kuwahara, H. Kawashima, T. Tsuruoka, and H. Tsuda, "Current-driven phase-change optical gate switch using indium–tin-oxide heater," Appl. Phys. Express **10**(7), 072201 (2017).

[59] H. Zhang, L. Zhou, L. Lu, J. Xu, N. Wang, H. Hu, B. M. A. Rahman, Z. Zhou, and J. Chen, "Miniature multilevel optical memristive switch using phase change material," ACS Photonics **6**(9), 2205–2212 (2019).

[60] Z. Fang, R. Chen, J. Zheng, A. I. Khan, K. M. Neilson, S. J. Geiger, D. M. Callahan, M. G. Moebius, A. Saxena, M. E. Chen, C. Rios, J. Hu, E. Pop, and A. Majumdar, "Ultra-low-energy programmable non-volatile silicon photonics based on phase-change materials with graphene heaters," Nat. Nanotechnol. **17**, 842 (2022).

[61] C. Ríos, Y. Zhang, M. Y. Shalaginov, S. Deckoff-Jones, H. Wang, S. An, H. Zhang, M. Kang, K. A. Richardson, C. Roberts, J. B. Chou, V. Liberman, S. A.

Vitale, J. Kong, T. Gu, and J. Hu, "Multi-level electro-thermal switching of optical phase-change materials using graphene," Adv. Photonics Res. **2**(1), 2000034 (2021).

[62]Y. Zhang, C. Fowler, J. Liang, B. Azhar, M. Y. Shalaginov, S. Deckoff-Jones, S. An, J. B. Chou, C. M. Roberts, V. Liberman, M. Kang, C. Ríos, K. A. Richardson, C. Rivero-Baleine, T. Gu, H. Zhang, and J. Hu, "Electrically reconfigurable non-volatile metasurface using low-loss optical phase-change material," Nat. Nanotechnol. **16**(6), 661–666 (2021).

[63]Y. Wang, P. Landreman, D. Schoen, K. Okabe, A. Marshall, U. Celano, H.-S. P. Wong, J. Park, and M. L. Brongersma, "Electrical tuning of phase-change antennas and metasurfaces," Nat. Nanotechnol. **16**, 667 (2021).

[64]S. Abdollahramezani, O. Hemmatyar, M. Taghinejad, H. Taghinejad, A. Krasnok, A. A. Eftekhar, C. Teichrib, S. Deshmukh, M. A. El-Sayed, E. Pop, M. Wuttig, A. Alù, W. Cai, and A. Adibi, "Electrically driven reprogrammable phase-change metasurface reaching 80% efficiency," Nat. Commun. **13**(1), 1696 (2022).

[65]Q. Wang, E. T. F. Rogers, B. Gholipour, C.-M. Wang, G. Yuan, J. Teng, and N. I. Zheludev, "Optically reconfigurable metasurfaces and photonic devices based on phase change materials," Nat. Photonics **10**(1), 60–65 (2016).

[66]A. Leitis, A. Heßler, S. Wahl, M. Wuttig, T. Taubner, A. Tittl, and H. Altug, "All-dielectric programmable Huygens' metasurfaces," Adv. Funct. Mater. **30**(19), 1910259 (2020).

[67]C. Williams, M. N. Julian, S. Borg, S. Bartram, and H. J. Kim, "Reversible optical tuning of GeSbTe phase-change metasurface spectral filters for mid-wave infrared imaging," Optica **7**(7), 746–754 (2020).

[68]H. Liu, W. Dong, H. Wang, L. Lu, Q. Ruan, Y. S. Tan, R. E. Simpson, and J. K. W. Yang, "Rewritable color nanoprints in antimony trisulfide films," Sci. Adv. **6**(51), eabb7171 (2020).

[69]S. Abdollahramezani, O. Hemmatyar, H. Taghinejad, A. Krasnok, Y. Kiarashinejad, M. Zandehshahvar, A. Alù, and A. Adibi, "Tunable nanophotonics enabled by chalcogenide phase-change materials," Nanophotonics **9**(5), 1189–1241 (2020).

[70]P. Praveen, T. P. Rose, and K. J. Saji, "Top electrode dependent resistive switching in M/ZnO/ITO memristors, M = Al, ITO, Cu, and Au," Microelectr. J. **121**, 105388 (2022).

[71]A. Sawa, "Resistive switching in transition metal oxides," Mater. Today **11**(6), 28–36 (2008).

[72]K. M. Kim, D. S. Jeong, and C. S. Hwang, "Nanofilamentary resistive switching in binary oxide system; a review on the present status and outlook," Nanotechnology **22**(25), 254002 (2011).

[73]H. Jiang, L. Han, P. Lin, Z. Wang, M. H. Jang, Q. Wu, M. Barnell, J. J. Yang, H. L. Xin, and Q. Xia, "Sub-10 nm Ta channel responsible for superior performance of a HfO₂ memristor," Sci. Rep. **6**(1), 28525 (2016).

[74]J. Joshua Yang, F. Miao, M. D. Pickett, D. A. A. Ohlberg, D. R. Stewart, C. N. Lau, and R. S. Williams, "The mechanism of electroforming of metal oxide memristive switches," Nanotechnology **20**(21), 215201 (2009).

[75]J. J. Yang, D. B. Strukov, and D. R. Stewart, "Memristive devices for computing," Nat. Nanotechnol. **8**(1), 13–24 (2013).

[76]J. J. Yang, M.-X. Zhang, J. P. Strachan, F. Miao, M. D. Pickett, R. D. Kelley, G. Medeiros-Ribeiro, and R. S. Williams, "High switching endurance in TaOx memristive devices," Appl. Phys. Lett. **97**(23), 232102 (2010).

[77]C. Hoessbacher, Y. Fedoryshyn, A. Emboras, A. Melikyan, M. Kohl, D. Hillerkuss, C. Hafner, and J. Leuthold, "The plasmonic memristor: A latching optical switch," Optica **1**(4), 198–202 (2014).

[78]A. Emboras, J. Niegemann, P. Ma, C. Haffner, A. Pedersen, M. Luisier, C. Hafner, T. Schimmel, and J. Leuthold, "Atomic scale plasmonic switch," Nano Lett. **16**(1), 709–714 (2016).

[79]E. Battal, A. Ozcan, and A. K. Okyay, "Resistive switching-based electro-optical modulation," Adv. Opt. Mater. **2**(12), 1149–1154 (2014).

[80]B. J. Choi, A. C. Torrezan, J. P. Strachan, P. G. Kotula, A. J. Lohn, M. J. Marinella, Z. Li, R. S. Williams, and J. J. Yang, "High-speed and low-energy nitride memristors," Adv. Funct. Mater. **26**(29), 5290–5296 (2016).

[81]N. Youngblood, C. A. Ríos Ocampo, W. H. P. Pernice, and H. Bhaskaran, "Integrated optical memristors," Nat. Photonics **17**, 561 (2023).

[82]A. Emboras, A. Alabastri, F. Ducry, B. Cheng, Y. Salamin, P. Ma, S. Andermatt, B. Baeuerle, A. Josten, C. Hafner, M. Luisier, P. Nordlander, and J. Leuthold,

"Atomic scale photodetection enabled by a memristive junction," ACS Nano **12**(7), 6706–6713 (2018).

[83]K. Portner, M. Schmuck, P. Lehmann, C. Weilenmann, C. Haffner, P. Ma, J. Leuthold, M. Luisier, and A. Emboras, "Analog nanoscale electro-optical synapses for neuromorphic computing applications," ACS Nano **15**(9), 14776–14785 (2021).

[84]G. Di Martino, S. Tappertzhofen, S. Hofmann, and J. Baumberg, "Nanoscale plasmon-enhanced spectroscopy in memristive switches," Small **12**(10), 1334–1341 (2016).

[85]Z. Fang, B. Tossoun, A. Descos, D. Liang, X. Huang, G. Kurczveil, A. Majumdar, and R. G. Beausoleil, "Fast and energy-efficient non-volatile III-V-on-silicon photonic phase shifter based on memristors," arXiv:2305.14271 (2023).

[86]M. Grajower, N. Mazurski, J. Shappir, and U. Levy, "Non-volatile silicon photonics using nanoscale flash memory technology," Laser Photonics Rev. **12**(4), 1700190 (2018).

[87]Y. Li, H. Yu, H. Dai, J. Jiang, G. Wang, L. Yang, W. Wang, J. Yang, and X. Jiang, "Graphene-based floating-gate nonvolatile optical switch," IEEE Photonics Technol. Lett. **28**(3), 284–287 (2016).

[88]J. Parra, I. Olivares, A. Brimont, and P. Sanchis, "Non-volatile epsilon-near-zero readout memory," Opt. Lett. **44**(16), 3932–3935 (2019).

[89]S. Cheung, D. Liang, Y. Yuan, Y. Peng, Y. Hu, G. Kurczveil, and R. G. Beausoleil, "Non-volatile heterogeneous III-V/Si photonics via optical charge-trap memory," arXiv:2305.17578 (2023).

[90]J.-F. Song, A. E.-J. Lim, X.-S. Luo, Q. Fang, C. Li, L. X. Jia, X.-G. Tu, Y. Huang, H.-F. Zhou, T.-Y. Liow, and G.-Q. Lo, "Silicon photonic integrated circuits with electrically programmable non-volatile memory functions," Opt. Express **24**(19), 21744–21751 (2016).

[91]Y. Li, W. Chen, T. Dai, and P. Wang, "Nonvolatile integrated optical phase shifter with flash memory technology," Appl. Phys. Express **12**(10), 102005 (2019).

[92]I. Olivares, J. Parra, and P. Sanchis, "Non-volatile photonic memory based on a SAHAS configuration," IEEE Photonics J. **13**(2), 4600108 (2021).

[93]K.-H. Kim, I. Karpov, R. H. Olsson, and D. Jariwala, "Wurtzite and fluorite ferroelectric materials for electronic memory," Nat. Nanotechnol. **18**(5), 422–441 (2023).

[94]A. I. Khan, A. Keshavarzi, and S. Datta, "The future of ferroelectric field-effect transistor technology," Nat. Electron. **3**(10), 588–597 (2020).

[95]R. Waser, *Nanoelectronics and Information Technology: Advanced Electronic Materials and Novel Devices* (John Wiley & Sons, 2012).

[96]K. Alexander, J. P. George, J. Verbist, K. Neyts, B. Kuyken, D. Van Thourhout, and J. Beeckman, "Nanophotonic Pockels modulators on a silicon nitride platform," Nat. Commun. **9**(1), 3444 (2018).

[97]S. Abel, F. Eltes, J. E. Ortmann, A. Messner, P. Castera, T. Wagner, D. Urbonas, A. Rosa, A. M. Gutierrez, D. Tulli, P. Ma, B. Baeuerle, A. Josten, W. Heni, D. Caimi, L. Czornomaz, A. A. Demkov, J. Leuthold, P. Sanchis, and J. Fompeyrine, "Large Pockels effect in micro- and nanostructured barium titanate integrated on silicon," Nat. Mater. **18**(1), 42–47 (2019).

[98]K. Sakayori, Y. Matsui, H. Abe, E. Nakamura, M. Kenmoku, T. Hara, D. Ishikawa, A. Kokubu, K. Hirota, and T. I. Takuro Ikeda, "Curie temperature of BaTiO₃," Jpn. J. Appl. Phys. **34**(9S), 5443 (1995).

[99]S. S. P. Parkin, C. Kaiser, A. Panchula, P. M. Rice, B. Hughes, M. Samant, and S.-H. Yang, "Giant tunnelling magnetoresistance at room temperature with MgO (100) tunnel barriers," Nat. Mater. **3**(12), 862–867 (2004).

[100]D. Apalkov, A. Khvalkovskiy, S. Watts, V. Nikitin, X. Tang, D. Lottis, K. Moon, X. Luo, E. Chen, A. Ong, A. Driskill-Smith, and M. Krounbi, "Spin-transfer torque magnetic random access memory (STT-MRAM)," J. Emerging Technol. Comput. Syst. **9**(2), 13-1-13-35 (2013).

[101]A. Makarov, *Modeling of Emerging Resistive Switching Based Memory Cells* Institute for Microelectronics (TU, Wien, Vienna, 2014).

[102]S. Cueff, J. John, Z. Zhang, J. Parra, J. Sun, R. Orobtchouk, S. Ramanathan, and P. Sanchis, "VO₂ nanophotonics," APL Photonics **5**(11), 110901 (2020).

[103]P. Markov, R. E. Marvel, H. J. Conley, K. J. Miller, R. F. Haglund Jr., and S. M. Weiss, "Optically monitored electrical switching in VO₂," ACS Photonics **2**(8), 1175–1182 (2015).

[104]A. Tripathi, J. John, S. Kruk, Z. Zhang, H. S. Nguyen, L. Berguiga, P. R. Romeo, R. Orobtchouk, S. Ramanathan, Y. Kivshar, and S. Cueff, "Tunable Mie-resonant

dielectric metasurfaces based on VO₂ phase-transition materials," ACS Photonics **8**(4), 1206–1213 (2021).

[105] M. Stegmaier, C. Ríos, H. Bhaskaran, C. D. Wright, and W. H. P. Pernice, "Nonvolatile all-optical 1 × 2 switch for chipscale photonic networks," Adv. Opt. Mater. **5**(1), 1600346 (2017).

[106] C. Ríos, Q. Du, Y. Zhang, C.-C. Popescu, M. Y. Shalaginov, P. Miller, C. Roberts, M. Kang, K. A. Richardson, T. Gu, S. A. Vitale, and J. Hu, "Ultra-compact nonvolatile phase shifter based on electrically reprogrammable transparent phase change materials," PhotoniX **3**(1), 26 (2022).

[107] Z. Fang, J. Zheng, A. Saxena, J. Whitehead, Y. Chen, and A. Majumdar, "Nonvolatile reconfigurable integrated photonics enabled by broadband low-loss phase change material," Adv. Opt. Mater. **9**(9), 2002049 (2021).

[108] R. Chen, Z. Fang, C. Perez, F. Miller, K. Kumari, A. Saxena, J. Zheng, S. J. Geiger, K. E. Goodson, and A. Majumdar, "Non-volatile electrically programmable integrated photonics with a 5-bit operation," arXiv:2301.00468, (2023).

[109] F. Eltes, G. E. Villarreal-Garcia, D. Caimi, H. Siegwart, A. A. Gentile, A. Hart, P. Stark, G. D. Marshall, M. G. Thompson, J. Barreto, J. Fompeyrine, and S. Abel, "An integrated optical modulator operating at cryogenic temperatures," Nat. Mater. **19**(11), 1164–1168 (2020).

[110] P. Xu, J. Zheng, J. K. Doylend, and A. Majumdar, "Low-loss and broadband nonvolatile phase-change directional coupler switches," ACS Photonics **6**(2), 553–557 (2019).

[111] S. S. Saseendran, T. D. Kongnyuy, B. Figeys, K. J. Sundar, J. P. Soulie, D. Goosens, S. Kundu, R. Jansen, X. Rottenberg, and P. Soussan, in *2022 IEEE Photonics Conference (IPC)* (IEEE, 2022), pp. 1–2.

[112] M. Wei, K. Xu, B. Tang, J. Li, Y. Yun, P. Zhang, Y. Wu, K. Bao, K. Lei, Z. Chen, H. Ma, C. Sun, R. Liu, M. Li, L. Li, and H. Lin, "'Zero change' platform for monolithic back-end-of-line integration of phase change materials in silicon photonics," arXiv:2308.15723 (2023).

[113] K. Taki, N. Sekine, K. Watanabe, Y. Miyatake, T. Akazawa, H. Sakumoto, K. Toprasertpong, S. Takagi, and M. Takenaka, "Non-volatile optical phase shift in ferroelectric hafnium zirconium oxide," arXiv:2309.01967 (2023).

[114] W. Yan, Y. Yang, S. Liu, Y. Zhang, S. Xia, T. Kang, W. Yang, J. Qin, L. Deng, and L. Bi, "Waveguide-integrated high-performance magneto-optical isolators and circulators on silicon nitride platforms," Optica **7**(11), 1555–1562 (2020).

[115] P. Pintus, L. Ranzani, S. Pinna, D. Huang, M. V. Gustafsson, F. Karinou, G. A. Casula, Y. Shoji, Y. Takamura, T. Mizumoto, M. Soltani, and J. E. Bowers, "An integrated magneto-optic modulator for cryogenic applications," Nat. Electron. **5**(9), 604–610 (2022).

26 October 2023 02:57:41